PROGRESS IN INTEGRATION OF REMOTE SENSING–DERIVED FLOOD EXTENT AND STAGE DATA AND HYDRAULIC MODELS

Guy Schumann,[1] Paul D. Bates,[1] Matthew S. Horritt,[2] Patrick Matgen,[3] and Florian Pappenberger[4]

[1] The ability to monitor floods with sensors mounted on aircraft and satellites has been known for decades. Early launches of satellites and the availability of aerial photography allowed investigation of the potential to support flood monitoring from as far as space. There have been notable studies on integrating data from these instruments with flood modeling since the late 1990s. There is now a consensus among space agencies to strengthen the support that satellites can offer. This trend has stimulated more research in this area, and significant progress has been achieved in recent years in fostering our understanding of the ways in which remote sensing can support or even advance flood modeling. This research goes considerably further than using a wet/dry flood map for model validation as in early studies of this type. Therefore, this paper aims to review recent and current efforts to aid advancing flood inundation modeling from space.

Citation: Schumann, G., P. D. Bates, M. S. Horritt, P. Matgen, and F. Pappenberger (2009), Progress in integration of remote sensing–derived flood extent and stage data and hydraulic models, *Rev. Geophys.*, *47*, RG4001, doi:10.1029/2008RG000274.

1. INTRODUCTION

[2] With flood frequency likely to increase as a result of altered precipitation patterns triggered by climate change [*Drogue et al.*, 2004], there is a growing demand for more data and, at the same time, improved flood inundation modeling. The aim is to develop more reliable flood-forecasting systems over large scales that account for uncertainty in observations, modeling, and output. Over the last few decades, there have been major advances in the fields of remote sensing, particularly microwave remote sensing, and flood inundation modeling. However, until recently, progress within both fields has been largely separate without any clear connection. Joining both research fields with a stronger integration of remote sensing of flood information and hydraulic modeling has only emerged over the last decade as a result of significant advances in synthetic aperture radar (SAR) remote sensing techniques and high-performance computing encouraging a boost in distributed flood modeling, with uncertainty. Given these recent efforts, there is a need for an up-to-date review on integrating remote sensing with hydraulic modeling.

[3] Furthermore, the two most notable reviews on this topic date back to 1997 [*Smith*, 1997; *Bates et al.*, 1997], but since then, progress in this area has been significant. Recent research papers on integrating remote sensing with flood modeling have studied (1) the retrieval and modeling of flood hydrology information from remote sensing observations (e.g., discharge, flood extent and area, and water stage), (2) the use of these data to calibrate and validate hydrodynamic models, (3) the potential of remote sensing to understand and improve model structures, and (4) the usefulness of remote sensing data assimilation with models. In all of these studies, uncertainty in observations as well as model parameters and predictions has been a major aspect. All these research efforts have contributed significantly to the recent advances in this area. Hence, it is the aim of this paper to provide the research community with a thorough review of progress in the combined field of remote sensing and flood modeling achieved over the last decade. In doing so, we highlight that over the last decade (radar) remote sensing has emerged as a powerful tool to support and advance flood modeling. The paper will report on recent progress in the integration of remote sensing–derived flood extent with topographic data for water stage retrieval with the aim to incorporate and assimilate these data with flood models. This complements recent reviews by *Alsdorf et al.* [2007] on spaceborne remote sensing of freshwaters and direct water level measurement (i.e., altimetry and interfer-

[1]School of Geographical Sciences, University of Bristol, Bristol, UK.
[2]Halcrow Group Ltd., Swindon, UK.
[3]Department of Environment and Agro-Biotechnologies, CRP–Gabriel Lippmann, Belvaux, Luxembourg.
[4]European Centre for Medium-Range Weather Forecasts, Reading, UK.

ometry) and by *Marcus and Fonstad* [2008] on optical remote sensing of floods. Also, reviews on discharge retrieval from space have been done extensively by *Bjerklie et al.* [2003] and *Smith and Pavelsky* [2008].

2. REMOTE SENSING OF FLOOD EXTENT AND STAGE

[4] Probably the most reliable source of remotely sensed flood area and extent data is aerial photography [see, e.g., *Yu and Lane*, 2006]. However, because of the elevated cost associated with airborne acquisitions, satellites are often regarded as an inviting alternative for flood monitoring and management [see, e.g., *MacIntosh and Profeti*, 1995; *Profeti and Macintosh*, 1997; *Zhou et al.*, 2000; *Sanyal and Lu*, 2004]. Nevertheless, given its higher accuracy and reliability, the use of aerial photography for flood applications is worth mentioning. The ability to acquire useful information about water from space has been known since the late 1970s with the availability of images from the Earth Resources Technology Satellite [*McGinnis and Rango*, 1975] and Landsat series [*Bhavsar*, 1984]. Very rapidly, the strengths of spaceborne radar imaging for flood monitoring (e.g., penetration of clouds, insensitivity to weather [see, e.g., *Sanyal and Lu*, 2004], and ability to acquire data during day and night) became obvious [*Imhoff et al.*, 1986]. This section provides a review of the various methods that exist to map flood extent and area from aerial photography and spaceborne radar imagery and integrate these with other sources of information to obtain water stage.

2.1. Flood Extent and Area Mapping

[5] Given the very high spatial resolution of the imagery, flood extent is derived from color or panchromatic aerial photography by digitizing the boundaries at the contrasting land-water interface. A very simple and straightforward approach to retrieving useful flood information from space is that of extracting a binary map consisting of dry and flooded pixels. This procedure is applied throughout the world by many research teams and engineering and consulting companies as well as emergency response services and governmental institutions. The most appealing mode of acquisition of a flood image is, for obvious reasons, with visible and thermal bands. Flood mapping with such imagery has met some success [*Marcus and Fonstad*, 2008]; however, the systematic application of such techniques is hampered by persistent cloud cover during floods, particularly in small to medium-sized catchments where floods often recede before weather conditions improve. Also, the inability to map flooding beneath vegetation canopies, as demonstrated by, e.g., *Hess et al.* [1995, 2003] and *Wilson et al.* [2007] with radar imagery, limits the applicability of optical sensors. Given the limitations of these sensors to acquire flood information routinely, flood detection and monitoring seems realistically only feasible with microwave (i.e., radar) remote sensing, as microwaves penetrate cloud cover and are reflected away from the sensor by smooth open water bodies.

[6] The use of passive microwave systems over land surfaces is difficult given the large angular beams of such systems [*Rees*, 2001] resulting in spatial resolutions as large as 20–100 km. Interpretation of the wide range of materials with many different emissivities is thus rendered nearly impossible. Nevertheless, as the sensor is sensitive to changes in the dielectric constant, very large areas of water, for instance, can be detected [*Sippel et al.*, 1998; *Jin*, 1999; *Melack et al.*, 2004], but their uncertainties may be large [*Papa et al.*, 2006].

[7] Active microwave imagery from SAR seems to be at the moment the only reliable source of information for monitoring floods on rivers <1 km in width. According to *Blyth* [1997], the spatial resolution from current spaceborne SAR sensors (i.e., 25–30 m) should satisfy requirements for most applications. Furthermore, Blyth stated that satellite data with a ground resolution of 100 m would be of value for rapid response requirements for floods on large rivers, but he found no evidence to support this claim. Indeed, the need for rapid dissemination of information is probably of greater importance in the first instance than the production of a high-resolution product [*Blyth*, 1997]. For example, *Di Baldassarre et al.* [2009] demonstrate that inundation width derived from a 75 m resolution SAR image in wide swath mode (delivered 24 h after an event on the Po River, Italy, in early June 2008) can be used in near real time to verify timely flood inundation modeling. Obviously, near-real-time availability of higher-resolution SAR data is preferred, but the cost of such data becomes an important part of the equation [*Blyth*, 1997].

[8] Many SAR image-processing techniques exist to more or less successfully derive flood area or extent [*Aplin et al.*, 1999], including simple visual interpretation [*MacIntosh and Profeti*, 1995; *Oberstadler et al.*, 1997; *Brivio et al.*, 2002], image histogram thresholding [e.g., *Brivio et al.*, 2002; *Matgen et al.*, 2004; *Schumann et al.*, 2005], automatic classification algorithms [e.g., *Hess et al.*, 1995; *Bonn and Dixon*, 2005], image texture algorithms [*Schumann et al.*, 2005], and multitemporal change detection methods [e.g., *Calabresi*, 1995; *Laugier et al.*, 1997; *Delmeire*, 1997], of which extensive reviews are provided by *Liu et al.* [2004] and *Lu et al.* [2004]. Complex autologistic regression [*Atkinson*, 2000] and principal component analysis to model the degree of correlation between multiple images [*Matgen et al.*, 2006] may also be applied. Image statistics-based active contour models [*Horritt*, 1999] have been used by *Bates et al.* [1997], *Horritt* [1999], *De Roo et al.* [1999], *Horritt et al.* [2001], and *Schumann et al.* [2005]. This approach, also termed a "snake" [*Horritt*, 1999], starts as a vector on the river centerline and grows outward to finally settle at contrasting boundaries, i.e., the flood extent. Figure 1 illustrates the flooded area extracted from a RADARSAT-1 image using the snake approach and from an ERS-2 image thresholded into wet/dry/undetermined classes.

[9] Classification inaccuracies of flooded areas (i.e., dry areas mapped as flooded and vice versa) vary considerably because of (1) inappropriate image-processing algorithms as
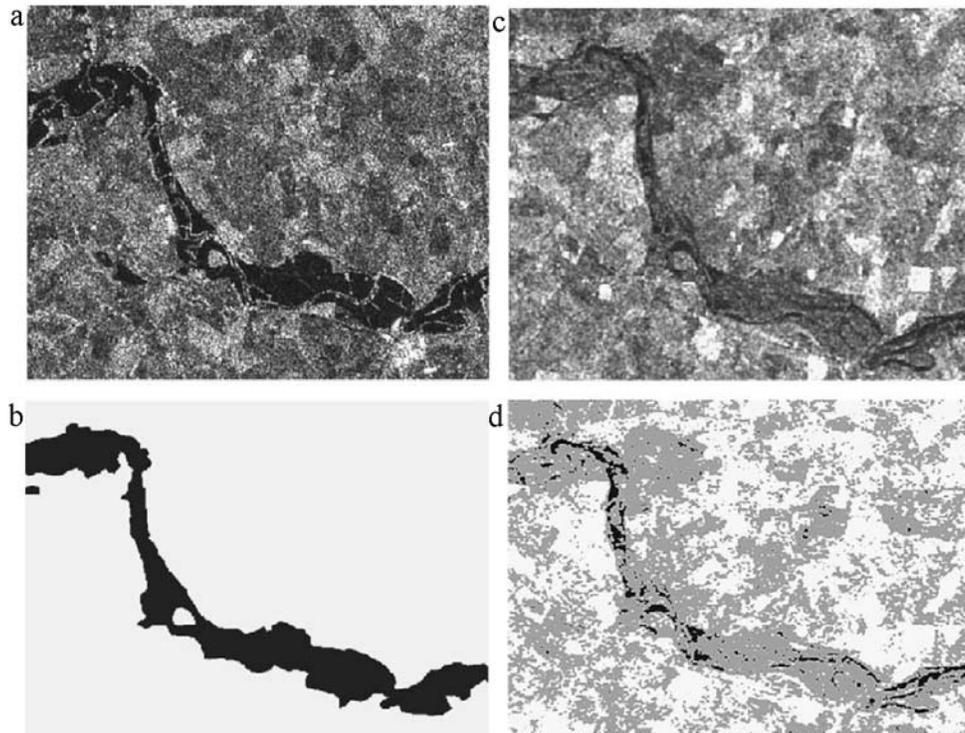
Figure 1. Details of SAR imagery and classification results. (a) The RADARSAT image (courtesy of the Canadian Space Agency) is segmented using the active contour model to give the (b) inundation extent. (c) The noisier ERS-2 imagery (courtesy of the European Space Agency) is thresholded into (d) wet/dry/undetermined classes. Top left coordinates of each plot are 52°41′34″N, 2°41′29″W. Reprinted from *Horritt* [2006], copyright 2006, with permission from Elsevier.

illustrated by *Schumann et al.* [2005], who assessed the effect of uncertainty in binary flood maps as a result of different algorithms on flood model calibration; (2) altered backscatter characteristics; (3) unsuitable wavelength and/or polarizations; (4) unsuccessful multiplicative noise (i.e., speckle) filtering; (5) remaining geometric distortions; and (6) inaccurate image geocoding. *Horritt et al.* [2001] state that wind roughening and the effects of vegetation protruding above the water surface, both of which may produce significant pulse returns, complicate the imaging of the water surface. However, it is noteworthy that *Hess et al.* [1990] have reviewed the usefulness of the double-bounce reflection caused by smooth water surfaces below vegetation canopies to map flooding in forested and vegetated areas, such as wetlands [*Hess et al.*, 1995, 2003; *Wilson et al.*, 2007]. Also, because of the corner reflection principle [*Rees*, 2001] in conjunction with coarse ground resolution, SAR is currently unable to extract flooding from urban areas, which, for obvious reasons, would be desirable when using remote sensing for flood management. The magnitudes of such errors are a function of spatial resolution, wavelength, radar look angle, and polarization. *Bates et al.* [2006], for example, compare RADARSAT and airborne SAR imagery and conclude that although airborne SAR may not change views of floodplain inundation processes, it does allow a more detailed understanding than has hitherto been possible and allows an ability to quantify basic parameters (floodplain storage volumes and dewatering

rates) for the first time. *Horritt and Bates* [2002] compare RADARSAT and ERS for flood sensing and comment on differences due to look angle. *Henry et al.* [2006] compare different polarizations (vertically sent and vertically received, horizontally sent and vertically received, and horizontally sent and horizontally received (HH)) for flood mapping purposes and conclude that HH is most efficient in distinguishing flooded areas. *De Roo et al.* [1999] identify the geometric correction and geocoding (or orthorectification) of a SAR image as the most difficult and time-consuming step in the entire image-processing chain.

2.2. Indirect Water Stage Retrieval

[10] Apart from using direct measuring techniques from space [*Alsdorf et al.*, 2007], river stage can also be estimated at the land-water interface, using high spatial resolution satellite or airborne imagery or aerial photography in combination with topographic maps or a digital elevation model (DEM) [*Smith*, 1997]. Given that high-resolution DEMs (e.g., from scanning laser altimetry) are becoming more readily available, if flood boundaries can be adequately extracted from SAR or other remote sensing imagery, it is possible to map not only flood extent but also derive water stage at the shoreline and flow depth across the floodplain for a given event. As early as the 1980s there were several successful attempts to derive water stages or heights from remote sensing data sets in such a way [e.g., *Currey*, 1977; *Gupta and Banerji*, 1985]. In general, accuracies of the
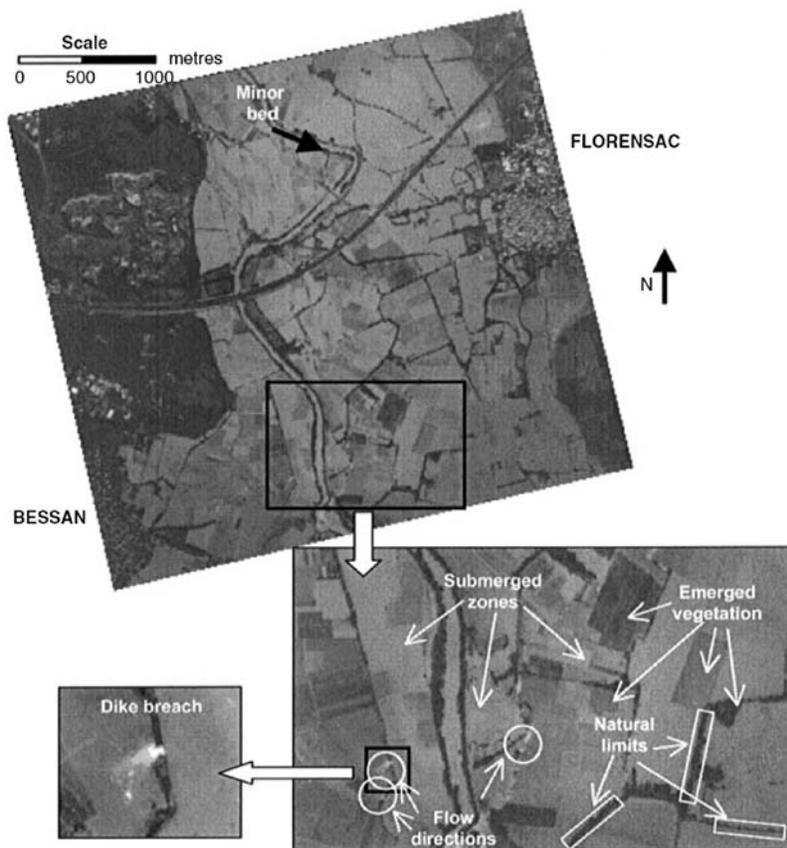
Figure 2. Example of an aerial photograph of a flood on the Hérault River (France) in early November 1994 (top left coordinates are 43°23′36″N, 3°25′18″E). Extracted information includes natural limits, submerged or emerged vegetation, and flow directions. Taken from *Puech and Raclot* [2002], copyright 2002, John Wiley and Sons, Ltd., reproduced with permission.

resulting water stages or heights increase with the complexity of the method and the horizontal and vertical resolution of the data sets used. Other than a straightforward and rather simple overlay operation between a remote sensing–derived flood extent and a DEM, more consistent remote sensing–based water stage modeling can be adopted.

2.2.1. Water Stages From Aerial Photography

[11] Some interesting developments in extracting water levels from remote sensing are those which integrate topographic data [*Raclot*, 2006]. The resolution of data acquired from airborne platforms is still significantly better than that currently possible using satellite-based sensors [*Lane et al.*, 2003]. Flood water boundaries can be plotted from aerial photographs and checked in the field by measuring distances to road corners, buildings, farm dams, fence lines, channels, and drains, for example. Topographic maps with small-interval contours and level data may provide an excellent ground truth check for water levels [*Currey*, 1977]. For water stage retrieval using remotely sensed very high resolution topographic data provided by light detecting and ranging (lidar) or photogrammetric data sets, *Lane et al.* [2003] use lines from flood deposits on aerial photographs.

[12] *Puech and Raclot* [2002; see also *Raclot and Puech*, 2003; *Raclot*, 2006] propose a rather complex methodology that is based on extensive fieldwork, hydraulic knowledge,

and aerial photography interpretation skills (see Figure 2). Similar to possible approaches with most 1-D hydrodynamic models, the floodplain is segmented into polygons in which water levels are supposed to be horizontal. In order to ensure a decreasing water trend with flow direction, extracted water stages are adjusted using an automated algorithm based on hydraulic constraints [*Puech and Raclot*, 2002]. Used in conjunction with topographic maps, interpretation of aerial photography followed by field measurement campaigns gives a vertical root mean squared error (RMSE) of ~20 cm. Despite these encouraging results, the technique seems difficult to adapt to SAR images because of their inappropriate spatial resolution and their relatively high level of distortions.

2.2.2. Water Stages From Satellite Radar Imagery

[13] Given the much coarser spatial resolution and the many sources of signal distortions associated with currently available radar imagery, the methods applied to aerial photography for water stage retrieval need to be adapted adequately. *Oberstadler et al.* [1997] used different observed flood boundaries on multiple ERS-1 images in conjunction with topographic contours to derive flood levels. *Brakenridge et al.* [1998] take this approach further by incorporating positional and altitudinal accuracy of topographic contour data and of the ERS-1 SAR image. A

comparison with a steady state hydraulic model simulation provided important information on the amplitude of the flood propagation wave. To improve the delineation of the shoreline in areas of flooded vegetation, *Horritt et al.* [2003] use vegetation heights derived from lidar data. This simple but efficient method permits better waterline height extraction. In a similar concept, *Mason et al.* [2007] use lidar height data to constrain an active contour model [*Horritt*, 1999; *Horritt et al.*, 2001] in order to improve flood delineation on SAR imagery.

[14] In a similar approach to that developed by *Puech and Raclot* [2002] for aerial photography, *Hostache et al.* [2005] apply a depth-mapping method to a SAR flood image using high-precision photogrammetric data. The method accounts for hydraulically sensitive zones and positional uncertainty of the SAR-derived flood map. They end up with an uncertainty between maximum and minimum water depth estimation of ~30 cm, on average. The application of the SAR-based method to a lower-magnitude flood event [*Hostache et al.*, 2009] resulted in an average uncertainty of 58 cm. This demonstrates that more complex image processing applied to moderate-resolution SAR provides results that are within the expected error bounds of the topographic data at hand (e.g., approximately ±20 cm for lidar), even for smaller-scale flood events. It might be argued that with a decrease in water stage accuracy, the information content decreases rapidly and is believed to dissipate at errors greater than half a meter, and as a result, hydrodynamic models might be ill conditioned if such inaccurate data are limited in number. Also, a change in water heights of half a meter or more will result in significantly larger changes in flood extent. Another approach to provide maximum and minimum water stage information is proposed by *Schumann et al.* [2008c], who extracted the mean height inside a buffer representing the uncertainty in the position of the flood boundaries.

[15] A remote sensing–based steady state (as satellite image acquisition is instantaneous and not continuous over time) flood-modeling approach has been proposed by *Matgen et al.* [2007a]. In a steady state regime, a system (in this case, flood flow) is modeled assuming that hydraulic demands and boundary conditions do not change with respect to time. *Matgen et al.* [2007a] propose to draw cross sections perpendicular to the river channel from which to extract elevation data from a high-resolution lidar DEM at the boundaries of the SAR-derived extent. A moving average filter is applied to the data to account for some of the noise associated with remotely sensed water heights. The SAR-based model estimates a smoothed linear trend of water levels either by using multiple regression analysis with *X* and *Y* map coordinates as the independent variables or by using a triangular irregular network generated from the "raw" remotely sensed water heights [*Matgen et al.*, 2007a]. Using this method the best vertical RMSE accuracy is 41 cm when validating the SAR model with field-based high water marks.

[16] An integrated and improved modeling approach to that adopted by *Matgen et al.* [2007a] was proposed by *Schumann et al.* [2007b]. Their model (Regression and Elevation Based Flood Information Extraction (REFIX)) uses linear, nonlinear, or piecewise linear regression on extracted water heights and stream centerline distance to derive spatially continuous (flood) water stages at the flood shoreline using intersection with a DEM, with respect to localized flow behavior. Apart from deriving spatially continuous water height from remote sensing, REFIX data can be used to produce a triangular irregular network mesh able to reliably map flood area, extent, and depth. *Schumann et al.* [2007b] show that flood depth can be mapped with an RMS accuracy of better than 20 cm, evaluated with spatially distributed high water marks measured in the field, but highlight the impact of the horizontal and vertical resolution of a DEM on the performance of the REFIX model as a major error source [*Schumann et al.*, 2008a].

[17] As regression modeling, particularly linear modeling, may be undesirable when integrated with more dynamic hydraulic models, *Schumann et al.* [2008b] have proposed to extract multiple water stage data points on river cross sections. This allows descriptive statistics (e.g., mean, median, or quartiles) to be applied at every river cross section instead of a least squares estimation (Figure 3). The advantage is that levels are now considered varying perpendicular to as well as in the direction of stream flow.

[18] Although the accuracy of topographic data is crucial, *LeFavour and Alsdorf* [2005] showed that globally and freely available DEMs from the Shuttle Topography Radar Mission (SRTM) flown in February 2000 may be used to extract surface water elevations and estimate a reliable surface water slope, provided that the river reach is long enough. *Kiel et al.* [2006] assessed the performance of X band and C band SRTM DEMs for the Amazon River and a smaller river in Ohio. They concluded that the C band SRTM DEM gives reliable water elevations also for smaller river reach lengths. They also state that while SRTM data are viable for hydrologic application, limitations such as the along-track antennae offset and the wide look angle suggest the necessity of a new satellite mission (Surface Water Ocean Topography (SWOT), http://swot.jpl.nasa.gov) for improved water elevation acquisition.

[19] In general, there is a trade-off between accuracy of the technique and either complexity of data processing or size and topographic complexity of the inundated floodplain. Inaccuracy is largely the result of a combination of the following two factors: (1) uncertain flood boundary position due to blurred signal response on the land-water contact zone and image geolocation errors and (2) coarse-resolution DEMs that might be inappropriate for the scale of the river reach under study.

[20] This section has shown that there has been significant progress in developing techniques to retrieve useful flood information from remote sensing data sets that is suitable for integration with hydraulic models. Also, current satellite missions (Table 1) are geared toward providing higher temporal and spatial resolution data for flood monitoring (see, for example, Figure 4) and to facilitate integration with models. Section 3 reviews recent progress in
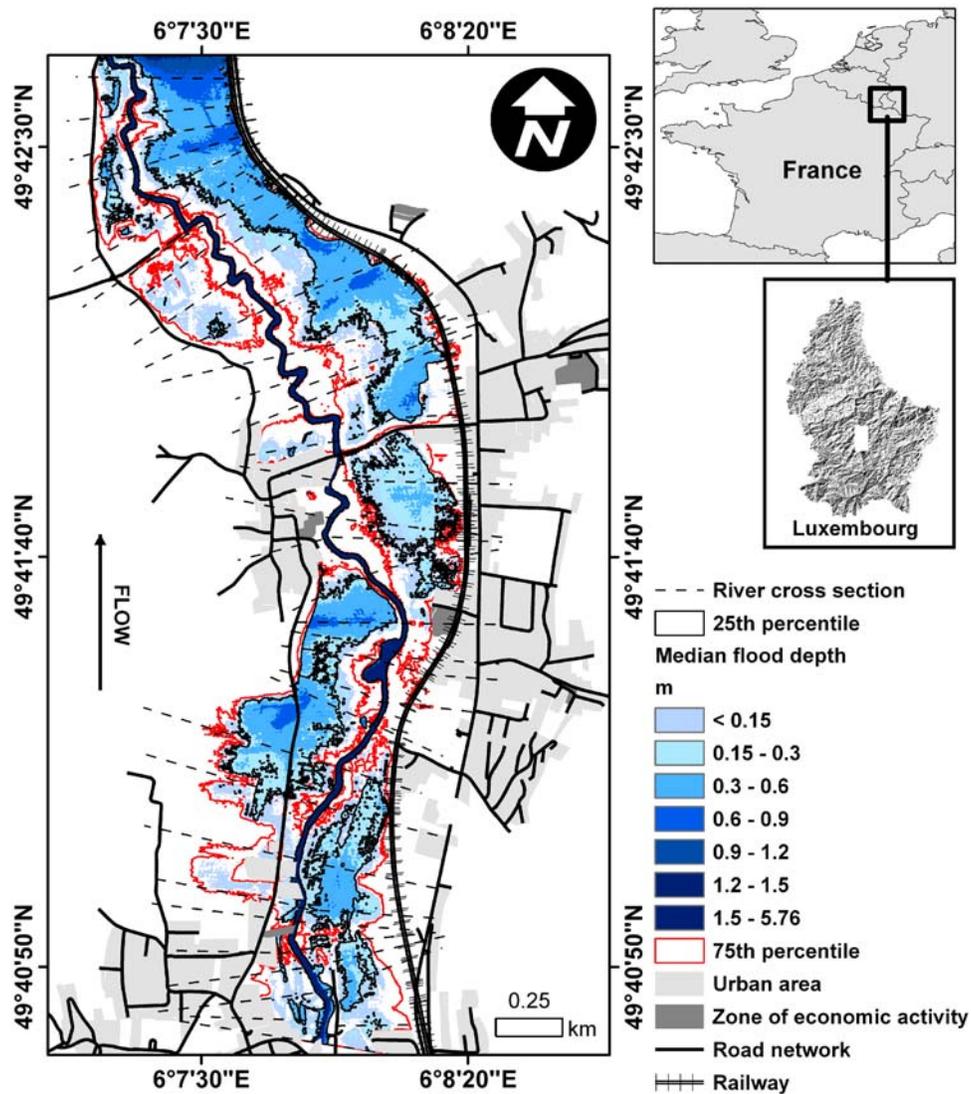
Figure 3. Flood depth and extent map conditioned on multiple cross-sectional water stages derived from a SAR flood extent of an event that occurred on the Alzette River (Grand Duchy of Luxembourg) in early January 2003.

integration of remotely sensed flood extent and stage data and hydraulic models.

3. INTEGRATION WITH HYDRAULIC MODELS

[21] The integration of remote sensing–derived flood information with models requires a profound understanding of the many factors underlying both the remote sensing and the flood-modeling part. For this reason, relatively few studies have looked at this complex interplay of these two fields. The common purpose of all the research studies reviewed here is to illustrate that remote sensing, in particular, spaceborne radar, can aid in advancing flood inundation modeling.

[22] Remote sensing provides information on both flood extent and stage, which can be used in real-time flood management, in building and understanding model structures, and in model calibration and evaluation. The different

information present in flood extents and stages means that different methods are required to integrate them with hydraulic modeling. The integration of flood extent and water stage data for real-time flood management will be discussed in section 4.

[23] The most common use of flood extent data in hydraulic modeling is for model calibration and evaluation (see, e.g., *Aronica et al.* [2002] as one of the classic studies on this). Calibration is here defined as adjusting model parameters (such as surface roughness or boundary conditions) to improve the fit between model predictions and observations. Validation, i.e., verification, involves comparing model output with observations and using this to draw conclusions about model performance.

[24] The processes of model calibration and validation with remotely sensed data involve some common steps: (1) extraction of flood extent or stages from the remote sensing data (see section 2) and (2) comparison with model predictions, using some form of performance measure. The
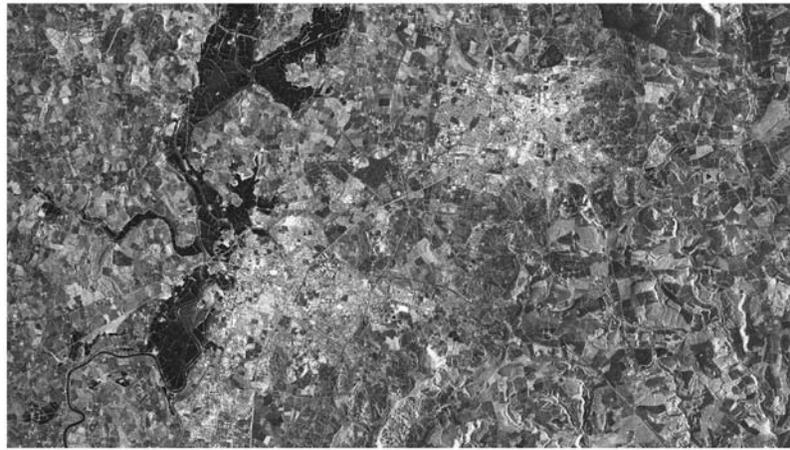
Figure 4. Subset of a TerraSAR-X (1 m) acquisition of the 2007 England floods. Taken on 25 July 2007, the image (top left coordinates are 51°56′47″N, 2°15′01″W) shows the towns of Gloucester (bottom) and Cheltenham (middle right) during the flood. Note that individual buildings inside the flooded area are easily identifiable, which might allow flood detection in urban areas with such high-resolution SAR imagery from space. Courtesy of German Aerospace Center.

difference between calibration and validation arises in how the performance measure is used. In calibration, the model parameters are adjusted to increase the performance, with the aim of finding an optimum set or range of parameters. In validation, we use the measure to assess model performance, compare models, and measure model improvements. Calibration and validation of a model are often strongly interconnected. Scarcity may dictate use of the same data for both calibration and validation, for example. Other than for model calibration or validation (i.e., quantifying model performance), remote sensing of floods may also help build, understand, and estimate model structures.

3.1. Building, Understanding, and Estimating Model Structures

[25] High-resolution remote sensing lidar data in the form of topography are the most widely used source of remote sensing data to build and condition flood inundation models

[e.g., *Marks and Bates*, 2000; *Lane and Chandler*, 2003; *Cobby et al.*, 2003]. lidar-derived vegetation height has been used by *Mason et al.* [2003] for floodplain friction (i.e., roughness) parameterization in two-dimensional river flood models. In a similar context, *Straatsma and Middelkoop* [2006] have segmented a floodplain into different friction classes using high-resolution vegetation data from airborne altimetry. Detailed information on floodplain land use types has been aggregated by *Werner et al.* [2005b] to form one, two, or five classes of floodplain roughness. Evaluating the identifiability of roughness in these classes showed complete insensitivity to floodplain friction in a flood inundation model (where floodplain friction sensitivity has a strong relationship with how dominant floodplain flow is for the reach, i.e., whether flow velocity in the floodplain is important, and how well floodplain processes are represented in a model). As a consequence, application of complex formulae to establish

TABLE 1. Current Satellite Missions Featuring SAR Sensors With High Potential for Flood Studies[a]

Mission (Agency, Year of Launch)	Sensor Frequency (Band, λ)	Polarization	Spatial Resolution (m)	Repeat Cycle[b] (Days)
ERS-2 (ESA, 1995)	5.3 GHz (C, 5.6 cm)	VV	25	35
RADARSAT-1 (CSA, 1995)	5.3 GHz (C, 5.6 cm)	HH	8–100	24
ENVISAT (ESA, 2002)	5.3 GHz (C, 5.6 cm)	VV-VH, VV-HV	12.5–1000	35
ALOS (JAXA, 2006)	1.3 GHz (L, 23.6 cm)	full	7–100	46
COSMO-SkyMed[c] (ASI, 2007)	9.6 GHz (X,[d] 3.1 cm)	dual	15–100	16
TerraSAR-X (DLR, 2007)	9.6 GHz (X, 3.1 cm)	full	1–16	11
RADARSAT-2 (MDA, ~2007)	5.3 GHz (C, 5.6 cm)	full	3–100	24

[a]Operating agency, year of launch, sensor frequency, mode of polarization, spatial resolution, and repeat cycle are also shown. ESA, European Space Agency; CSA, Canadian Space Agency; JAXA, Japan Aerospace Exploration Agency; ASI, Italian Space Agency; DLR, Germany Aerospace Center; MDA, MacDonald, Dettwiler, and Associates Ltd.; VV, vertically sent and vertically received; HH, horizontally sent and horizontally received; VH, vertically sent and horizontally received; HV, horizontally sent and vertically received.

[b]At highest spatial resolution. There is a strong inverse relationship between spatial resolution and repeat cycle (e.g., for RADARSAT-1 a daily repeat cycle is possible with a spatial resolution of 100 m). However, it is worth bearing in mind that timely acquisition can be programmed (tasked) for all satellites in case of emergency (usually, 24–48 h advance notice is required).

[c]This is a constellation of four SAR satellites operated by ASI and the Italian military. Although the orbit repeat cycle is 16 days, the constellation allows a very fast response time of only several hours.

[d]Multiband (X, C, L, and P) sensors are planned for the future.

roughness values for changed floodplain land use would seem inappropriate [*Werner et al.*, 2005b].

[26] Remotely sensed flood inundation extent contains information on hydraulic functioning of a river or floodplain, which can be used to build model structures (i.e., implementation of different roughness parameters, complexity in hydraulic structures and river cross section geometries, and detail of floodplain topography [see *Pappenberger et al.*, 2006]) and enhance process representation in the model. This goes beyond the calibration and evaluation process of section 3.2, which is mostly based on effective parameters. However, the two topics are related, as checks for hydraulic consistencies are performed within the calibration and evaluation process which are based on the remotely sensed image. In turn, the parameters of model structures which are identified by integrating remotely sensed flood inundation information are usually calibrated and evaluated at the same time. For example, *Schumann et al.* [2007b], as described in section 2, derived a procedure which uses radar imagery to extract the model structure and parameters for a simple flood inundation model. By combining radar images with a DEM the proposed stepped calibration procedure estimates model structures, in this particular case, simple linear regression, piecewise linear regressions, or nonlinear regression for the water surface, as well as the parameters of these models. The remotely sensed image is used to estimate not only parameters but also model structures. For example, it is possible to extract "hydraulic compartments," meaning areas in which the assumption of horizontal water levels is valid [*Hostache et al.*, 2009]. Additionally, a remotely sensed image would allow for the extraction of features on the floodplain or within the river. A very complex flood inundation model with one-dimensional flow paths, reservoirs, and specific boundary equations could be designed with this information (see *Raclot* [2006], as described in section 2).

[27] Integration of remotely sensed data has also been used to understand the difference in behavior of different model structures. For example, *Horritt et al.* [2007] have looked at the simple finite volume model and TELEMAC-2D showing differences in sensitivity of parameters, for example, channel roughness. *Schumann et al.* [2007a] have used localized error information, resulting from a comparison of model simulations with spatially distributed SAR-derived water stages, and attributed differences in model behavior to differences in channel roughness. This allowed the definition of a model structure that uses additional roughness parameters in order to strike the fine balance between model complexity and performance at the local level where accurate field observations are available. The study by *Schumann et al.* [2007a] illustrates well the close link between investigating model structures and evaluating model simulations.

3.2. Value of Remote Sensing in the Model Calibration-Validation Process

[28] Different remotely sensed data sets will be of different value in the modeling process. Two-dimensional maps of water stage, such as presented in Figure 3, could be expected to contain more information than a binary wet/dry map, for example, and hence provide a more exacting test of model performance. The difference in information content becomes less clear between a flood extent map and a discrete number of point stage measurements. The information content will also depend on the accuracy and precision of the observations, as a few accurate measurements may be of more use than a larger number of less accurate observations (see the conclusion of *Schumann et al.* [2008c]).

[29] The magnitude of the flood event observed is also significant. If the focus of the modeling study is flood prediction, observations of larger floods may be of greater value than smaller ones since it is desirable to test model performance against conditions as close as possible to those it is trying to predict. An exception to this is the use of flood extent observations for high flows constituting a "valley-filling" event. In this case, flood extent may show little sensitivity to hydraulics since the shoreline corresponds with higher topographic gradients bounding the floodplain, and a smaller flow may provide a better test of model performance. In the case of a "valley-filling event," errors in stage retrieval based on flood extent will also go up because of shoreline positional errors [see, e.g., *Schumann et al.*, 2008b]. Indeed, observations around bankfull discharge may be preferable, as flood extent may be very sensitive to water levels, and provide useful information on channel hydraulics. *Horritt et al.* [2007] have demonstrated this effect with multitemporal airborne radar imagery of the same flood event, with observations made during the receding limb of the hydrograph proving more effective at distinguishing models than imagery captured at peak flow.

[30] Care is required to ensure that the observations are providing useful information on the hydraulic processes that the model is trying to represent. Inundation patterns and stages during the drying phase may, for example, depend more on the microtopography or infiltration controlling the dewatering of isolated floodplain depressions rather than channel hydraulics. Similarly, during the wetting phase, flooding may be controlled by floodplain connectivity that is not represented in the hydraulic model. These effects may make little difference to peak water levels, and trying to force a model to reproduce them may be counterproductive.

3.3. Quantifying Model Performance

[31] There are many ways to evaluate the performance of flood inundation models in predicting flood extent or stage, and the choice of method will depend on the details of the model, observed data, and nature of the calibration or validation exercise. The most common approach in industry is to use a visual comparison. Visual comparison can be a powerful tool as a trained flood modeler not only checks for consistency between two images but also checks for hydraulic feasibility. The experienced modeler will also be able to weight observations according to their reliability, for example, paying less heed to observations where the results are known to be suspect, or to bias results toward areas of particular interest, such as risk concentrated in urban areas. Visual comparison techniques are, however, difficult to

TABLE 2. Contingency Table

	Present in Observation	Absent in Observation
Present in model	A	B
Absent in model	C	D

apply to a large set of images and will always produce a subjective assessment of model performance. Comparison of models validated against different data sets is particularly problematic.

[32] Quantitative measures allow an objective assessment of model performance. It is possible to compare different properties of the flood extent. For example, *Li and Wu* [2004] have demonstrated the comparison of landscape metrics that describe the spatial configuration of patterns, such as fragmentation, irregularity, or complexity of shape. However, the most common approach is a pixel-by-pixel approach.

3.3.1. Comparison of Binary Maps

[33] Binary comparison of maps is usually based on wet/dry cells [e.g., *Aronica et al.*, 2002; *Werner et al.*, 2005a; *Hunter et al.*, 2005; *Pappenberger et al.*, 2007]. Categorical

data often present fewer difficulties for model calibration studies given that the decision rule is a simple "yes/no" answer. An exhaustive comparison of different measures is provided in meteorology by *Stanski et al.* [1989] and has been reviewed for flood modeling by *Hunter* [2005], *Schumann et al.* [2005], and also *Pappenberger et al.* [2007]. The comparison is usually based on a contingency table (see Table 2), which reports the number of pixels correctly predicted as wet or dry, and underprediction and overprediction.

[34] *Hunter* [2005] and also *Pappenberger et al.* [2007] evaluated the properties of a wide range of binary measures, observing that while each of these area-based measures may be interpreted in a mathematical sense, their absolute values do not, in some cases, intuitively convey the degree of correspondence between a given model realization and a binary pattern observation. One solution to this problem is to provide a fuller description of prediction consistency using more methods of assessment, such as presented by *Pappenberger et al.* [2007], who correlated a fuzzy global performance measure with selected discrete binary performance measures for a set of LISFLOOD-FP model realizations to illustrate the differences between them. Table 3 summarizes the recommendations of *Hunter* [2005] for

TABLE 3. Recommendations for Various Measures[a]

Name	Comments	Equation[b]	Recommendation
Bias	Predictions that count (*A*, *B*, and *C*).	$\frac{A+B}{A+C}$	Recommended for summarizing aggregate model performance (i.e., underprediction or overprediction).
PC	Heavily influenced by the most common category and, hence, implicitly domain size.	$\frac{A+B}{A+B+C+D}$	Not recommended for either deterministic or uncertain calibration. The values for *D* are usually orders of magnitude larger than the other categories and may also be trivially easy to predict. Therefore, in many instances, PC will provide an overly optimistic assessment of model performance.
ROC analysis (*F* and *H*)	Artificial minimizing and maximizing of *F* and *H*, respectively.	$F = \frac{A}{A+C}$, $H = \frac{B}{B+D}$	Summarizes two different types of model error (i.e., underprediction or overprediction) that can occur and is potentially a useful tool for exploring their relative consequences and weighting in any subsequent risk analyses. Therefore, further consideration/development is required.
PSS	Underprediction *C*; relative magnitudes of *F* and *H*.	$\frac{(A \cdot D)-(C \cdot D)}{(B+D) \cdot (A+C)}$	Not recommended for either deterministic or uncertain calibration. Small *F* and large *H* are typical in flood applications, and, as such, the measure fails to adequately penalize overprediction. Significant overestimates of the flooded area are therefore only graded slightly poorer than optimal simulations. This also results in the preferential rejection of underpredicting parameter sets during uncertain calibration.
$F\langle 1 \rangle$	Correct predictions of flooding (*A*).	$\frac{A}{A+B+C}$	Recommended for both deterministic and uncertain calibration. A relatively unbiased measure that simply and equitably discriminates between underprediction and overprediction. As such, optimal simulations will provide the best compromise between these two undesirable attributes.
$F\langle 2 \rangle$	Overprediction (*B*).	$\frac{A-B}{A+B+C}$	Recommended for deterministic calibration (if underprediction is preferable). Explicitly penalizes overprediction but suffers as a result during uncertain calibration. Overpredicting simulations are wrongly retained to offset the bias introduced by the measure and provide an acceptable compromise between inundation map accuracy and precision. The benefits of rejection are reduced accordingly.
$F\langle 3 \rangle$	Underprediction.	$\frac{A-C}{A+B+C}$	Recommended for deterministic calibration (if overprediction is preferable). Here the measure was not tested within the uncertain calibration methodology. Though for other reaches, events, and study objectives, $F\langle 3 \rangle$ may provide a useful alternative to $F\langle 1 \rangle$ and $F\langle 2 \rangle$. It is not sensitive to domain size and appears to favor overprediction similar to PSS.

[a]After *Hunter* [2005]. PC, predicted correct; ROC, receiver operating characteristic; PSS, Peirce skill score.
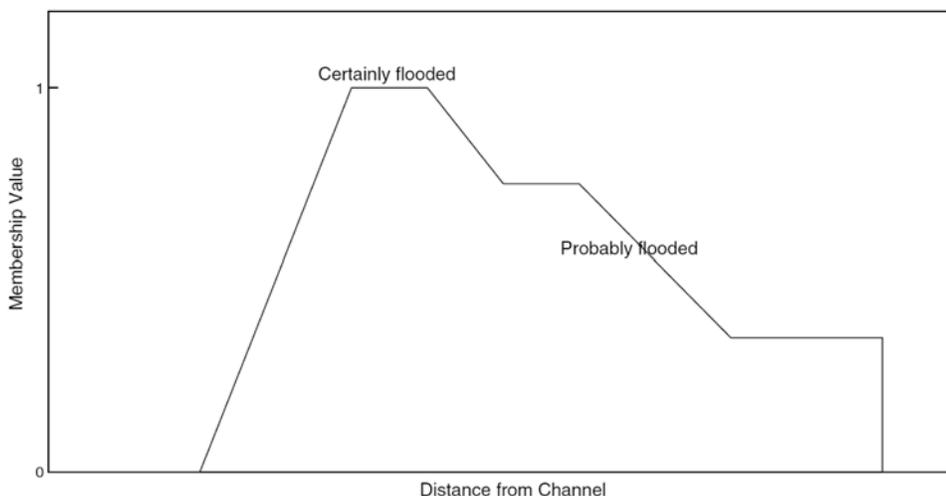[b]See Table 2.

Figure 5. Example of a membership function to compute the performance of inundation predictions at each river cross section. This function includes assumptions of the probability of pixels being flooded. The distance is given from the center of the river, and the membership values decrease toward the edges of the floodplain. Reprinted from *Pappenberger et al.* [2006], copyright 2006, with permission from Elsevier.

various measures. In this context, deterministic calibration means optimizing parameters of a particular model and establishing one parameter set. In uncertain calibration the performance measure is used to find multiple parameter sets that represent the system.

[35] *Schumann et al.* [2005] and *Hunter et al.* [2005] have both recommended the $F\langle 2 \rangle$ as the measure with the most potential in the discrete evaluation of flood inundation models. However, their analysis of the performance measure has been computed using inundation maps that were created using the snake algorithm [*Horritt*, 1999] to extract the flood outlines (in contrast to other methods, see section 2). The snake algorithm as well as the $F\langle 2 \rangle$ measure work better with large, continuous flooded areas than with "noisy," fragmented areas (see Figures 1b and 1d). Thus, the choice of a given binary performance measure is not an obvious one and needs to be based additionally on the type of floodplain and event.

[36] As an alternative to area-based performance measures, *Di Baldassarre et al.* [2009] evaluated a 1-D model in near real time using inundation width from a binary flood map extracted from a coarse-resolution SAR image in wide swath mode. The originality in this study is that fast image delivery followed by appropriate processing enabled timely verification of a calibrated model. Also, by using inundation width, the geolocation error becomes less important because there is no overlay operation involved as with a binary map comparison procedure. Furthermore, model assessment on the local scale is facilitated. This approach illustrates one possible way in which spaceborne remote sensing may support near-real-time flood management.

3.3.2. Comparison of Uncertain Flood Extent Observations

[37] Section 3.3.1 has briefly addressed the issue of optimization and uncertainty. In addition to the uncertainty in the hydraulic model one can also consider the uncertainty in the observations (see section 2 for some examples) in the

integration of flood extent and levels. *Matgen et al.* [2004] and also *Pappenberger et al.* [2006] have used a fuzzy membership approach to reflect the lack of knowledge about the real flood extent. A membership function allows one to express one's belief in a pixel being flooded and assign a performance value to a simulation which predicts the pixel as flooded accordingly. In both studies, a one-dimensional model was used, which predicted the flood extent at each river cross section, and the membership function was based on a distance to channel approach (see Figure 5). The shape of the membership function was based on Envisat advanced SAR (ASAR), ERS-2 SAR, and aerial photographs. As outlined in section 3.3.3, *Schumann et al.* [2008c] have chosen to use a variation of this fuzzy measure by defining a maximum and minimum water level at each cross section and computing the percentage of outliers for each simulation. The latter allows for a more clear analysis and understanding of the modeling results, as it reduces the complexity of the evaluation scheme, most likely without altering the conclusions.

[38] Methodologies to treat spatial fields in a similar way have also been developed. For instance, in the work by *Pappenberger et al.* [2007] a performance function is computed after *Hagen* [2003] by classifying the possibility of a cell being definitely flooded or not flooded (and two in-between classes). Thus, each cell represents four (fractional) values of membership classes, which are then compared to the model predictions which have been classified similarly. Similar to binary measures an average over the entire domain is computed to get an overall performance measure. *Pappenberger et al.* [2007] have shown that the measure compares well with traditional measures such as the binary measures in Table 3, but additionally, it includes the uncertainty in the observations and thus has the potential to include a higher information content.

[39] In contrast, *Horritt* [2006] has demonstrated that uncertain observed inundation data, while apparently
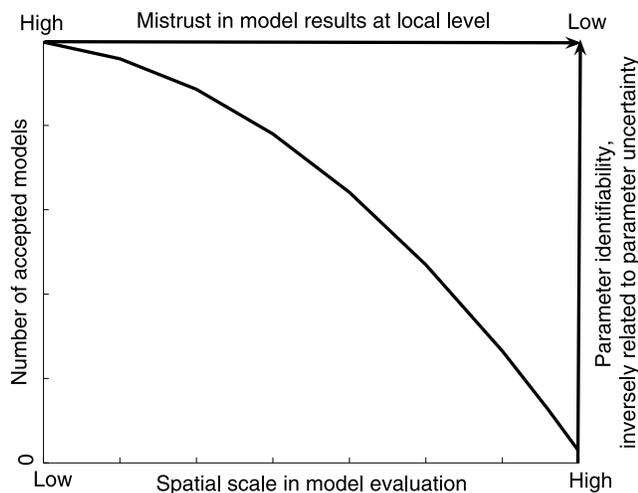
Figure 6. Representation of the effects of an increase in spatial scale in model evaluation on modeling results. From this relationship it may be concluded that (1) when moving toward higher spatial scales in model evaluation, both the number of accepted models and the model uncertainty decrease rapidly, unless more parameters are introduced to fit the local scale; (2) confidence in model results at the local level increases with an increase in spatial scale in model evaluation provided that observational uncertainty is not too high, as otherwise, moving toward higher evaluation scales has no effect; and (3) at a certain spatial scale (in the face of imperfect models), all models will inevitably be rejected, meaning that there are no acceptable predictions possible for the given reach with the model used. Taken from *Schumann et al.* [2008c], copyright 2008, International Association of Hydro-Environment Engineering and Research, reproduced with permission.

performing well in a calibration procedure, may reduce the predictive accuracy of uncertain flood models. In this context, *Schumann et al.* [2008c] point out that the definition of the error model on the observations has to be done very carefully as otherwise, doubtful predictions are derived. This argument illustrates that the performance measures formulated for understanding and calibration of a model may not be suitable in a real-time prediction approach.

[40] The recently introduced fuzzy set approach can be used to compare "distributions" of forecasted and observed flood extent data. However, it is based on classifying the individual pixels into memberships of discrete categories (possibility of being flooded). A powerful approach based on the Student's *t* test, which does not require this classification, has been presented by *Mason et al.* [2009] for water levels extracted from a SAR image using a lidar-corrected snake approach.

3.3.3. Comparison of Uncertain Water Levels

[41] Other than flood extent or area, model simulations can be compared to remote sensing–derived water levels, the retrieval of which is reviewed in section 2. Despite the fact that *Werner et al.* [2005a] have demonstrated that water depth is able to constrain the uncertainty in flood inundation models more efficiently than binary patterns, the number of

studies that refer to the use of remote sensing water levels in the model calibration or validation processes are, at present, very limited [*Schumann et al.*, 2007a, 2008c; *Hostache et al.*, 2009; *Mason et al.*, 2009]. The main reason is probably because until recently, the integration of accurately derived flood extents from a SAR image with topographic data to retrieve water stages has lacked precision. This inaccuracy has largely been the result of a combination of uncertain flood boundary position and DEMs that are inappropriate for the scale of the river reach under study. However, with the availability of lidar and recently developed innovative stage retrieval techniques (as described in section 2), this has considerably improved and, with the newly launched higher-resolution SAR sensors, is likely to continue.

[42] Recently, *Schumann et al.* [2007a] proposed a methodology that makes use of water stages from SAR to define additional flood model parameter classes according to different magnitudes of model error (see earlier in this section). This highlights the importance of model evaluation at the local scale. In a similar approach, *Mason et al.* [2009] used the Student's *t* test on the error information between SAR-derived waterlines and modeled ones to define model performances with an a priori defined uncertainty level.

[43] Another useful implementation is to use maximum and minimum water stages from SAR to set a spatially continuous interval inside which model simulations are required to fall in order to be considered acceptable [*Beven*, 2006]. Two slightly different approaches to the same problem using SAR-derived water stages are provided by *Schumann et al.* [2008c] and *Hostache et al.* [2009], who both show that such intervals enable the user to assess model performance at different spatial scales and to reject less reliable model simulations that are still retained with less abundant field data. Additionally, *Schumann et al.* [2008c] have shown that this evaluation procedure allows the modeler to establish the relationship between (1) the number of accepted models at different spatial scales, (2) the associated model uncertainty, and (3) the lack of confidence in model results at the local level (see Figure 6).

[44] With the launch of new radar satellites (e.g., RADARSAT-2, ALOS, COSMO-SkyMed, and TerraSAR-X) that have better spatial and radiometric resolutions, the uncertainties of water level estimates will presumably be further reduced, getting closer to the results of *Puech and Raclot* [2002] or *Raclot* [2006] obtained with aerial photographs [*Hostache et al.*, 2009].

[45] Another interesting potential of remote sensing–derived water levels, other than for model calibration or validation, is assimilation into models in the field of flood forecasting, which is reviewed in section 4.

3.3.4. Comparison of Uncertain Flood Predictions

[46] One important aim of integrating remotely sensed flood inundation into the modeling chain is to produce maps of inundation. A deterministic model simulation calibrated with a single remotely sensed flood inundation image will lead to a deterministic flood inundation map, which can be directly used for planning, model evaluation, or other purposes. However, if uncertainty is included into this
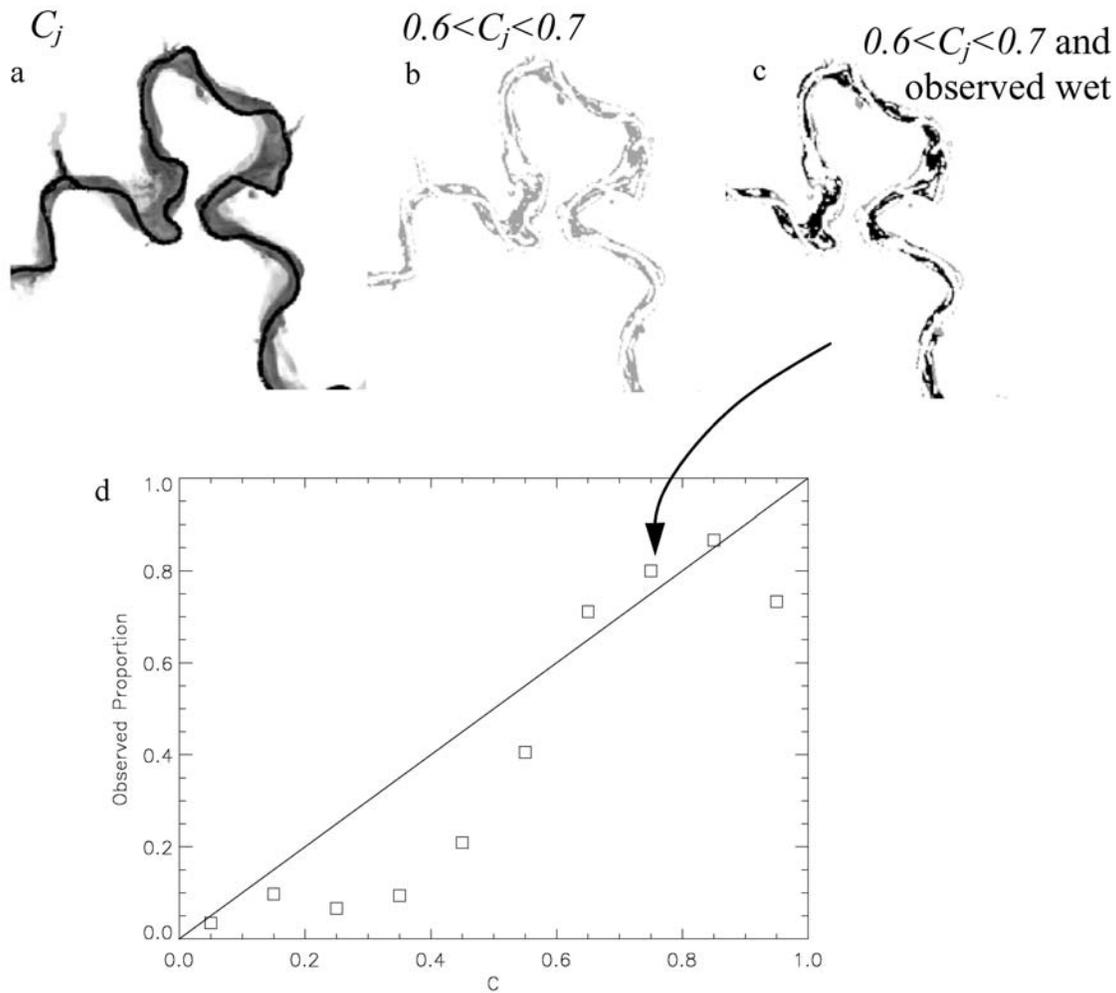
Figure 7. The reliability diagram. (a) The uncertain prediction is classified into (b) areas of similar C_j, then (c) the ratio of observed wet/dry cells is calculated. These then make up (d) the reliability plot, with a reliable model being one with points close to the 1:1 line. Reprinted from *Horritt* [2006], copyright 2006, with permission from Elsevier.

process and one deals with multiple simulations, then an uncertain output map has to be derived. *Romanowicz et al.* [1996] proposed the derivation of a "probability" map by

$$\text{RCM}_j = \frac{\sum_i L_i w_{ij}}{\sum_i L_i}, \qquad (1)$$

in which L_i is the weight for each simulation i and the simulation results for the jth model element (e.g., computational cell or node) are $w_{ij} = 1$ for wet and $w_{ij} = 0$ for dry. The weight can be based on normalized performance measures which are derived from maps conditioned on remotely sensed information. RCM_j is the relative confidence measure for each cell j, which expresses a belief that an uncertain prediction is a consistent representation of the system behavior (for a discussion, see *Hunter* [2005]).

[47] The evaluation of model predictions based on an optimal parameter set is conceptually simple, and the performance measure above may be used. However, it is more difficult to evaluate flood inundation predictions which lead to probabilistic type predictions and quantify a possibility of flooding for individual pixels. *Horritt* [2006] addressed this issue by exploiting the spatial nature of floods and computing model precision and accuracy over the model domain. A precise map will contain large areas which are classified as definitely dry or wet and few areas of probability around 0.5. The precision of the map can therefore be measured by the entropy (defined as C by *Horritt* [2006]). For an accurate uncertain map, the regions with probability 0.5, for example, will contain equal areas of wet and dry observations. The accuracy can therefore be visualized by the reliability curve, which plots the model probability against the proportions of wet and dry areas in the observations (see Figure 7). An accurate model will exhibit a 1:1 relationship, and the deviation from this (e.g., the RMS error) can be used as a measure of the accuracy. *Horritt* [2006] showed that both measures need to be applied, as otherwise, misleading conclusions can be drawn. The usage of precision and accuracy at the model validation stage can provide important information on the added value

of remotely sensed images and remains currently the only methodology to deal with the issue of validating uncertain flood inundation maps.

4. FLOOD FORECASTING AND WATER STAGE ASSIMILATION

[48] Assimilation of remote sensing–derived water levels in flood-forecasting systems is still very much in its infancy [*Walker et al.*, 2003], and only a couple of proof-of-concept studies have been published [*Andreadis et al.*, 2007; *Matgen et al.*, 2007b; *Neal et al.*, 2009] on this subject so far. This can be explained by a lack of maturity of processing chains needed to systematically extract hydraulically relevant information from remote sensing data. Such data sets further need to be routinely available and are required to be directly related to state variables of flood inundation models. Research over the last decade has led to significant progress with respect to spatially distributed information that can be gained from remote sensing observations. Innovative processing chains have been presented (see section 2.2) and provide an enhancement and diversification of water level products from remote sensing. Moreover, significant progress has been achieved in appreciating the uncertainty that is associated with remote sensing–derived data.

[49] Given the fact that satellite constellations with polar orbits will never produce temporally continuous surface fields [*Andreadis et al.*, 2007], the continuity in time that is needed in flood forecasting and water resources monitoring applications based on satellite data is currently only possible through a sequential assimilation of remote sensing information with models. In an operational flood-forecasting context, the procedure is to sequentially analyze and interpret discrepancies between model and observations and to make use of the systematic availability of remote sensing–derived information to reduce the predictive uncertainty of a flood-forecasting system. Since forecasting systems (i.e., a sequence of atmospheric, hydrologic, and hydraulic modeling) are susceptible to errors not only in their parameterization but also in forcing data and model structure it can be argued that a periodic verification and eventual updating with satellite observations is useful. This is based on the assumption that remote sensing errors are smaller than simulation errors [*Arya et al.*, 1983] and that the continuous confrontation of model predictions with observations in a data assimilation system presents an opportunity to better understand physical processes and observation quality [*Walker*, 1999]. In flood-forecasting applications in particular, the model needs to predict extreme events whose magnitudes are often situated well beyond the magnitude observed during calibration events. It is thus sensible to believe that a better understanding of flood-generating mechanisms and, consequently, a model setup that is more consistent with observations are likely to produce better predictions of extreme events. As a matter of fact, in order to be of relevance to flood-forecasting systems, remote sensing technologies need to deliver information with sufficient quality to increase the skill of forecasting systems.

[50] As pointed out by *Walker* [1999], there is a challenge to merge the high temporal resolution of generally rather poor model predictions with the spatially comprehensive but limited remote sensing observations to yield the best possible model predictions. Despite these apparent advantages, to date, only point measurements of river stage and discharge are routinely assimilated in hydraulic models [*Madsen and Skotner*, 2005], whereas assimilation of remote sensing–derived data has proven its utility only in a couple of case studies [*Andreadis et al.*, 2007; *Matgen et al.*, 2007b; *Neal et al.*, 2009]. In the meteorological sciences, assimilation of key remote sensing data is more widespread and has led to significant improvements in the skill of atmospheric models [*Daley*, 1991]. Assimilation of remotely sensed soil moisture in hydrological models, although not yet used operationally, has also provided promising results in several studies [*Ottle and Vidal-Madjar*, 1994; *Pauwels et al.*, 2001; *Francois et al.*, 2003; *Matgen et al.*, 2006]. It can be argued that there is an analogy between assimilation of remotely sensed soil moisture in hydrological models and remotely sensed surface water storage in flood inundation models. In fact, soil moisture and surface water both represent time-varying state data that can easily be related to prognostic states in forecasting systems. In both types of models, data assimilation can be used as a means to correct for errors in forcing.

[51] Building on knowledge derived from hydrologic and meteorologic data assimilation experience, various data assimilation techniques might be envisaged. The objective of data assimilation schemes is to put the model in better agreement with observed data whenever new observations become available. Data assimilation presents a strategy that allows extending satellite observations in time by sequentially updating flood inundation models using distributed water stages obtained from remote sensing. One might distinguish between direct insertion methods and more sophisticated ''optimal'' assimilation approaches, generally based on an ensemble Kalman filter (EnKF) [*Madsen and Canizares*, 1999; *Reichle et al.*, 2002; *Neal et al.*, 2007]. The former should only be applied if the uncertainties of the observations are much smaller than those of the simulations. The latter appears to be preferable when observations are susceptible to significant errors themselves, which is generally the case with remote sensing–derived data. However, uncertainties of both the simulations and observations need to be thoroughly appreciated before envisaging statistical assimilation approaches. The work of *Schumann et al.* [2008b] on the uncertainty of remotely sensed water stages is quite significant in this respect. Conceptually, sequential state updating is preferable to sequential parameter updating because parameter updating would violate a basic principle of physically based modeling, namely, that the constants should stay constant while the variables vary [*Kirchner*, 2006]. State updating is based on the assumption that errors in forcing data are the most significant sources of uncertainty in flood inundation modeling.
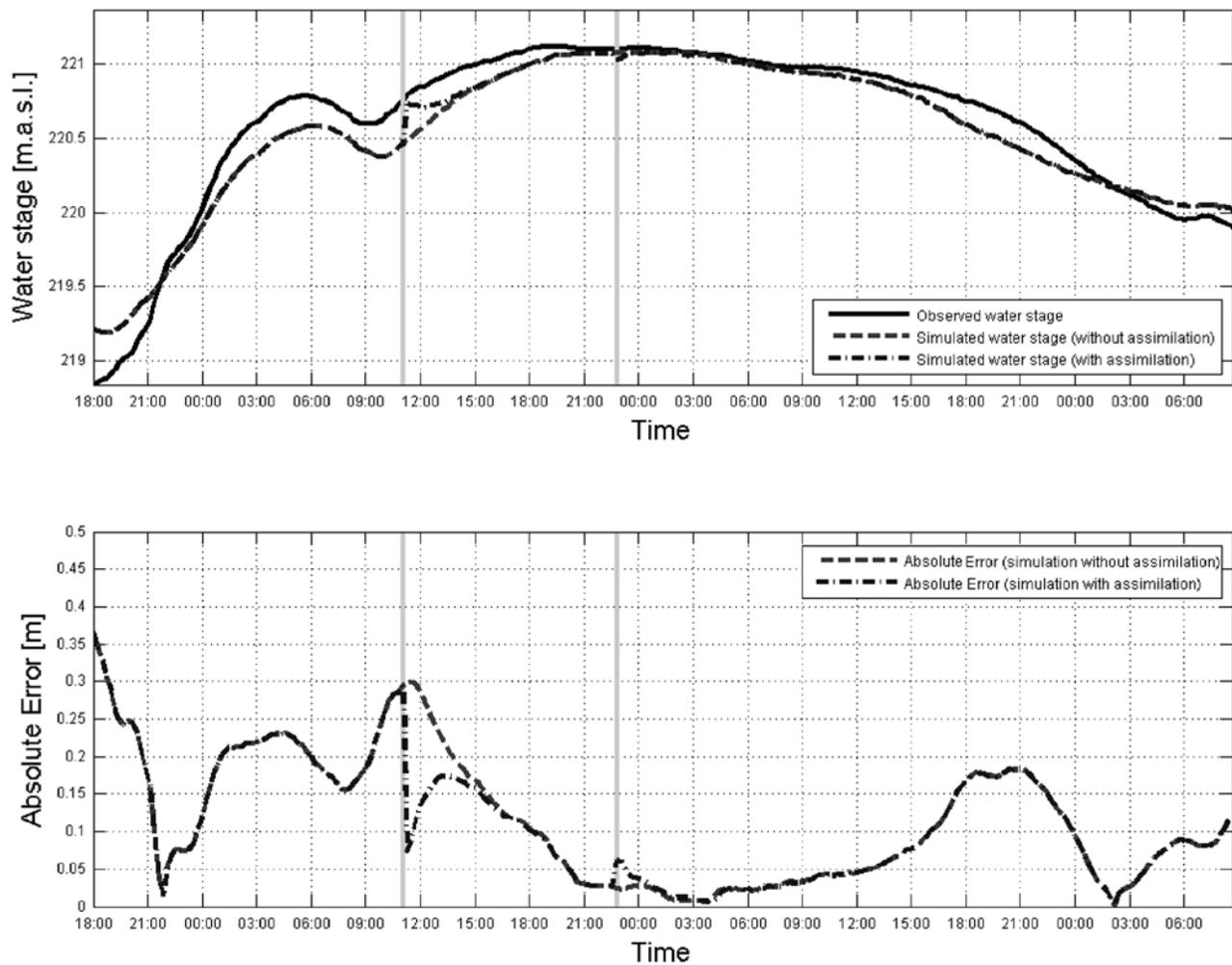
Figure 8. (top) Simulated water stages with and without data assimilation. The vertical lines depict the timing of the remotely sensed assimilation data. (bottom) The error between simulated and observed water stages with and without data assimilation.

[52] In the study of *Matgen et al.* [2007b], which follows a direct insertion strategy, the state of the model that represents the storage of water in the channel and floodplain is verified with remote sensing–derived water surface lines. The prognostic state of the model is forced at each cross section to fall within a previously computed uncertainty interval of remote sensing–derived water stages. After the model is conditioned on the observed data, it evolves again freely until the next observation becomes available. The approach was tested with ENVISAT ASAR and ERS-2 SAR imagery acquired during a flood event on the Alzette River (Grand Duchy of Luxembourg). The results of the study demonstrated that radar flood images have the potential to lead to improved flood inundation modeling. However, in a state-updating framework, the value of the remote sensing information decreases rapidly because the effect of the assimilation of remote sensing information is limited by the persistence of the initial condition (see Figure 8). Indeed, the time efficiency of data acquisition and processing determines to a large extent the usefulness of remotely sensed information. It has been shown that several hours after image acquisition the remote sensing observations no

longer provided any substantial improvement to the flood-forecasting system. Furthermore, the authors demonstrated that the large intervals of uncertainty that are typical for remote sensing–derived water stages tend to bracket model predictions at any time and at any place, meaning that no correction or additional information may be obtained from remote sensing.

[53] *Andreadis et al.* [2007] came to similar conclusions in their proof-of-concept study. While *Matgen et al.* [2007b] adopted a direct insertion approach, *Andreadis et al.* [2007] used a "design scenario" assimilation approach based on the assumption of an a priori knowledge of observation and simulation errors and found that a square root version of the EnKF was able to recover water depth and discharge from a corrupted flood inundation simulation by assimilating synthetic water surface level observations. At each assimilation step the hydrodynamic model was used in conjunction with remote sensing data to find an optimal estimate of the water surface line. A persistent improvement of the forecast skill is hampered by the fact that during subsequent time steps the model is again dragged toward the "preupdate" simulated water depth with respect to the upstream boundary

condition. To tackle this problem, the authors adopted a state augmentation approach that consists of complementing the state-updating approach with an update of the boundary condition, thereby correcting errors in forcing data as part of the data assimilation scheme. *Andreadis et al.* [2007] used a hydrologic model to estimate streamflow at the upstream boundary of their flood inundation model. Remotely sensed water stages enable the computation of the error in forcing terms that are assumed to be correlated in time. By applying an autoregressive model to simulate errors in the boundary condition between satellite overpasses, the skill of the forecasting system can be improved in a more persistent way. When the boundary condition is not the result of a hydrologic model but is obtained from direct measurements of water stage, the method has to be slightly adapted. *Pappenberger et al.* [2006] showed that the boundary condition, and thus the stage discharge (i.e., rating curve) parameters, have a significant impact on inundation predictions and that it is important to take account of the uncertainty in using rating curves for flood inundation models. One approach to solve this issue is to appreciate the uncertainty of the rating curve that is used to convert the precise water stage measurement into a comparatively uncertain discharge and to find the optimal estimate of stage and flow using a state augmentation approach as described above. *Neal et al.* [2009] generated an ensemble of flood imulations with discharge estimations from a simple rainfall-runoff model forced with precipitation estimates from numerical weather predictions. They then demonstrated that discharge values can be updated with real case (as opposed to synthetic) water levels derived from spaceborne SAR imagery using an EnKF.

[54] In conclusion, the pioneer studies in the field of assimilation of remote sensing data in flood-forecasting systems have faced a number of considerable challenges. In all three studies, errors in the upstream boundary inflow [*Andreadis et al.*, 2007; *Matgen et al.*, 2007b; *Neal et al.*, 2009] were considered the only sources of model error, and other likely sources of model uncertainty such as channel and floodplain roughness, channel and floodplain topography, and model structure were neglected. There is a consensus that a mere reinitialization of hydrodynamic models with distributed water stages obtained from remote sensing does not lead to significant improvement because of the dominating effect of the forcing terms on the modeling results. By sequentially confronting models with remote sensing observations it becomes possible to "diagnose" what is wrong in the latest model setup and to find out how modeling can be improved to find a better agreement with satellite observations. In this respect, the use of error forecasting models as advocated by *Andreadis et al.* [2007] and also *Neal et al.* [2007] in the context of spatially distributed gage measurements seems to indicate a promising way forward. Although reinitialization through state updating may help to temporarily reduce the uncertainties in hydrodynamic modeling, a significant and persistent improvement can only be obtained by looking for, and identifying, the reasons that cause disagreement between model results and observations. It needs to be the

objective to identify and correct components that are responsible for the discrepancy between modeled and observed variables. It may be argued that such a "diagnostic approach" [*Gupta et al.*, 2008] ensures the most efficient usage of remote sensing observations in flood modeling. It is reasonable to assume that the apparent distance between the observed and simulated water surface line might indicate that some aspect of the model setup is invalid. Obviously, it is important to adequately understand all the different error sources and relationships between them, as otherwise, it is impossible to conduct the model development in a meaningful way. Since flood inundation models are calibrated with data of a past flood event, the potential reasons for a mismatch are indeed numerous: the rating curve used to describe the boundary condition might become erroneous from a certain magnitude of inflow onward, model parameters (i.e., channel and floodplain roughness values) may vary with time (e.g., because of vegetation growth), important intermediate inflows may have been neglected, or the model structure may become inappropriate with increased inflow. In any case, if a model proves to be invalid with respect to new observation data, it needs improvement.

5. FUTURE NEEDS

[55] With respect to data assimilation in hydrodynamic models, water stage products inferred from remote sensing need to become more mature. More essentially, though, there is a clear need to move toward a systematic monitoring of floods at a global scale. As of today, revisit times of radar satellites can take up to 35 days, and image delivery and processing is feasible in 24–48 h. *Andreadis et al.* [2007] showed that the performance of a virtual remote sensing assimilation system degraded substantially as the interval between successive satellite overpasses increased. With the numerous recent and upcoming SAR satellite missions and promising multisensor constellations (e.g., SWOT, ALOS, RADARSAT-2, TerraSAR-X, COSMO-SkyMed, and Sentinel-1), timelier image delivery will be possible, and a new era of SAR-derived flood services can be envisaged. To ensure data availability is compatible with near-real-time data assimilation, new processing chains need to be developed. A possible way forward is provided by the new SWOT mission that uses radar altimetry and SRTM-type technology for timely water level recording at a global scale. Also, the European Space Agency's new Fast Access to Imagery for Rapid Exploitation tool which is integrated into a grid-based environment (Grid Processing on Demand, http://gpod.eo.esa.int/) [see also *Fusco et al.*, 2005] is promising. An alternative is to use the forecasting capability of a flood-forecasting system to order satellite imagery of the predicted event 48 h in advance [*Aplin et al.*, 1999] or to apply for a programmable acquisition. There is no doubt that a comprehensive remote sensing data assimilation framework has the potential of becoming a critical component in future flood-forecasting systems.

[56] In addition to more systematic radar observations, a number of other developments are also required to make

possible a more comprehensive integration of models and remotely sensed flood extent and water height data. First, in many locations around the globe floodplain terrain data are insufficiently accurate or not consistently available to support modeling. Despite the progress in using lidar-derived DEMs for flood modeling [see, e.g., *Cobby et al.*, 2001], only SRTM data have global coverage and the potential to be used in some flood-modeling studies [e.g., *Wilson et al.*, 2007; *Sanders*, 2007; *Schumann et al.*, 2008a], despite typical vertical noise of approximately ±5 m. Here, too, the proposed SWOT satellite mission may provide the beginning of a solution as over time, repeated imaging of surface water extent and elevation can be used to build up detailed floodplain topography maps using the so-called "waterline" method [*Mason et al.*, 1998]. With a maximum repeat time of ∼10 days this potentially equates to the retrieval of ∼75 floodplain topographic contours over the scheduled 3 year SWOT mission lifetime, thereby yielding an unprecedented wealth of detail concerning floodplain topographic features that can be used in inundation models.

[57] Second, and in a similar vein, global (or at least national) data sets on river channel bathymetry are required to accurately simulate channel flow occurring prior to overbank inundation. While considerable numbers of river surveys have been undertaken, these data are often fragmented, inconsistent, out of date, or not in the public domain. A possible solution here is to create a "level 1" data product based on river widths determined from satellite imagery [*Smith and Pavelsky*, 2008] and geomorphic relationships [e.g., *Leopold and Maddock*, 1953] to approximately estimate the channel depth. While crude, making such a data set public may lead local users to see an advantage in improving the coverage for their areas of interest. It may then be possible to capture these inputs using a "wiki" approach or other Web 2.0 methods to engage the collective power of the large river-modeling user community, as has recently been advocated by *Buytaert et al.* [2008] for hydrological modeling. Local users would be able to update sections of the data set on the basis of their detailed understanding, and the changes could be automatically tracked, commented upon, and, if necessary, revoked. In this way, too, a comprehensive metadata set could also be captured simultaneously.

[58] Lastly, a number of recent studies [e.g., *Bates et al.*, 2006; *Pappenberger et al.*, 2006] have shown that with fine spatial resolution (<3 m) topographic data accurate to <10 cm in the vertical, such as lidar and SAR-derived flood extent and water height data for model calibration, the largest (i.e., limiting) uncertainty in flood modeling is the discharge data used as model boundary condition forcing. This is confirmed by recent data assimilation studies [e.g., *Andreadis et al.*, 2007; *Neal et al.*, 2007; *Matgen et al.*, 2007b] which show that model predictions rapidly degrade after updating if the forcing data are not consistent with observed water levels. Here it is not just that data may be sparse or difficult to obtain but that currently available discharge measurement techniques become increasingly

unreliable under the high-flow conditions relevant to flood forecasting and inundation mapping. Here we need to develop new techniques to measure high flow discharge accurately and safely, better attention from national water authorities to the location of gaging sites, and a comprehensive effort to systematically and accurately generate rating curves applicable to high flows.

[59] As the recent history of this field has shown, development of new data sources will stimulate the creation of new models, analysis techniques, and assimilation methods, all facilitated by the increasing availability of multicore high-performance computers. These models and related approaches will need to be made fit for integration with remotely sensed data at scales ranging from local to global. At the core of these developments will also be a continuing need to focus on the calibration and validation of uncertain models against uncertain data to correctly evaluate risks in probabilistic terms. The parsimonious nature of flood inundation model parameterization compared to most other forms of environmental simulation is a distinct advantage here as only spatial fields of effective roughness parameters need to be estimated. However, the physics of energy loss processes in open channel flows are still not well understood, and our best available tools are lumped drag coefficients which have seen little theoretical development in the last 100 years. A fundamental research need is therefore to develop a comprehensive theory of "effective roughness" which accounts for variations in model structure and spatial scale.

6. CONCLUSIONS

[60] This paper has described and reviewed currently available remote sensing techniques to retrieve flood extent and water stages from space and subsequently try to integrate these with hydrodynamic models for a more rigorous evaluation of such models or improvement of uncertain flood inundation predictions. Microwave remote sensing for floods has the advantage over optical data of penetrating cloud and rain, features often associated with flooding. Moreover, data can be acquired independent of time of day. Although only univariate data, i.e., single waveband [*Aplin et al.*, 1999], SAR images can detect flooding with high spatial resolutions, different wavelengths, and incidence angles and in multiple polarization modes.

[61] Trying to obtain accurate flood extents and centimeter-scale accuracies in water stage estimation from remote sensing that are within expected accuracies of model predictions enables the modeler to evaluate and also improve uncertain flood inundation predictions from flood inundation models more readily and more rigorously, for instance, within an uncertainty framework, where multiple model predictions run with different parameter sets may be acceptable given uncertainty and errors in both model structure and observation data [*Beven and Binley*, 1992]. Acknowledging and examining the extent of uncertainty in

both data and model should be generally accepted as a key element in flood risk management exercises [*Pappenberger and Beven*, 2006]. Especially when integrating uncertain spatially distributed observation data such as derived from remote sensing with uncertain model structures, it is clear that uncertainty-based analysis is a welcomed paradigm.

[62] Combining remote sensing data capture techniques with hydraulic modeling has now become established as a powerful approach, the robustness of which needs, however, to be examined further, in particular for flood forecasting. What is certainly to be gained from this development is that fundamental research issues in terms of both model evaluation and remote sensing data processing techniques will be addressed in one way or another. In a very similar sense, *Cazenave et al.* [2004] argue that scientists have much to gain from current and future satellite observations and missions to provide (global) hydrological data sets that could be used to evaluate process models. Moreover, it is expected that satellite measurements combined with models that allow direct integration of such data would provide the basis for assimilation of remotely sensed data [*Alsdorf et al.*, 2005], for instance, in operational flood-forecasting systems.

[64] The Editor responsible for this paper was Peter Riley. He thanks Bret Sanders, two additional anonymous technical reviewers, and one anonymous cross-disciplinary reviewer.

REFERENCES

Alsdorf, D., E. Rodriguez, D. Lettenmaier, and J. Famiglietti (2005), WatER: The Water Elevation Recovery satellite mission—Response to the National Research Council Decadal Survey request for information, technical report, Ohio State Univ., Columbus. (Available at http://bprc.osu.edu/water/publications/WatER_NRC_RFI.pdf)

Alsdorf, D. E., E. Rodrguez, and D. P. Lettenmaier (2007), Measuring surface water from space, *Rev. Geophys.*, 45, RG2002, doi:10.1029/2006RG000197.

Andreadis, K. M., E. A. Clark, D. P. Lettenmaier, and D. E. Alsdorf (2007), Prospects for river discharge and depth estimation through assimilation of swath-altimetry into a raster-based hydrodynamics model, *Geophys. Res. Lett.*, 34, L10403, doi:10.1029/2007GL029721.

Aplin, P., P. M. Atkinson, A. R. Tatnall, M. E. Cutler, and I. M. Sargent (1999), SAR for flood monitoring and assessment, paper presented at Remote Sensing Society 1999: Earth Observation: From Data to Information, Remote Sens. Soc., Nottingham, U. K.

Aronica, G., P. D. Bates, and M. S. Horritt (2002), Assessing the uncertainty in distributed model predictions using observed binary pattern information within GLUE, *Hydrol. Processes*, 16, 2001–2016.

Arya, L. M., J. C. Richter, and J. F. Paris (1983), Estimating profile water storage from surface zone soil moisture measurements under bare field conditions, *Water Resour. Res.*, 19, 403–412.

Atkinson, P. M. (2000), Autologistic regression for flood zonation using SAR imagery, paper presented at 26th Annual Conference, Remote Sens. Soc., Leicester, U. K.

Bates, P. D., M. S. Horritt, C. N. Smith, and D. C. Mason (1997), Integrating remote sensing observations of flood hydrology and hydraulic modelling, *Hydrol. Processes*, 11, 1777–1795.

Bates, P. D., M. D. Wilson, M. S. Horritt, D. Mason, N. Holden, and A. Currie (2006), Reach scale floodplain inundation dynamics observed using airborne synthetic aperture radar imagery: Data analysis and modelling, *J. Hydrol.*, 328, 306–318.

Beven, K. (2006), A manifesto for the equifinality thesis, *J. Hydrol.*, 320, 18–36.

Beven, K., and A. Binley (1992), The future of distributed models: Model calibration and uncertainty prediction, *Hydrol. Processes*, 6, 279–298.

Bhavsar, P. (1984), Review of remote sensing applications in hydrology and water resources management in India, *Adv. Space Res.*, 4, 193–200.

Bjerklie, D. M., S. L. Dingman, C. J. Vorosmarty, C. H. Bolster, and R. G. Congalton (2003), Evaluating the potential for measuring river discharge from space, *J. Hydrol.*, 278, 17–38.

Blyth, K. (1997), Floodnet: A telenetwork for acquisition, processing and dissemination of Earth observation data for monitoring and emergency management of floods, *Hydrol. Processes*, 11, 1359–1375.

Bonn, F., and R. Dixon (2005), Monitoring flood extent and forecasting excess runoff risk with RADARSAT-1 data, *Nat. Hazards*, 35, 377–393.

Brakenridge, G. R., B. T. Tracy, and J. C. Knox (1998), Orbital SAR remote sensing of a river flood wave, *Int. J. Remote Sens.*, 19(7), 1439–1445.

Brivio, P. A., R. Colombo, M. Maggi, and R. Tomasoni (2002), Integration of remote sensing data and GIS for accurate mapping of flooded areas, *Int. J. Remote Sens.*, 23(3), 429–441.

Buytaert, W., D. Reusser, S. Krause, and J.-P. Renaud (2008), Why can't we do better than Topmodel?, *Hydrol. Processes*, 22, 4175–4179.

Calabresi, G. (1995), The use of ERS data for flood monitoring: An overall assessment, paper presented at 2nd ERS Applications Workshop, Eur. Space Agency, London.

Cazenave, A., P. Milly, H. Douville, J. Beneveniste, D. Lettenmaier, and P. Kosuth (2004), International workshop examines the role of space techniques to measure spatio-temporal change in terrestrial waters, *Eos Trans. AGU*, 85(6), 8.

Cobby, D. M., D. C. Mason, and I. J. Davenport (2001), Image processing of airborne scanning laser altimetry data for improved river flood modelling, *ISPRS J. Photogramm. Remote Sens.*, 56, 121–138.

Cobby, D. M., D. C. Mason, M. S. Horritt, and P. D. Bates (2003), Two-dimensional hydraulic flood modelling using a finite-element mesh decomposed according to vegetation and topographic features derived from airborne scanning laser altimetry, *Hydrol. Processes*, 17, 1979–2000.

Currey, D. T. (1977), Identifying flood water movement, *Remote Sens. Environ.*, 6, 51–61.

Daley, R. (1991), *Atmospheric Data Analysis*, Cambridge Univ. Press, Cambridge, U. K.

Delmeire, S. (1997), Use of ERS-1 data for the extraction of flooded areas, *Hydrol. Processes*, 11, 1393–1396.

De Roo, A., J. Van Der Knijff, M. Horritt, G. Schmuck, and S. De Jong (1999), Assessing flood damages of the 1997 Oder flood and the 1995 Meuse flood, paper presented at 2nd International ITC Symposium on Operationalization of Remote Sensing, Int. Inst. for Geo-Inf. Sci. and Earth Obs., Enschede, Netherlands.

Di Baldassarre, G., G. Schumann, and P. Bates (2009), Near real time satellite imagery to support and verify timely flood modelling, *Hydrol. Processes*, 23, 799–803.

Drogue, G., L. Pfister, T. Leviandier, A. El Idrissi, J. F. Iffly, P. Matgen, J. Humbert, and L. Hoffmann (2004), Simulating the spatio-temporal variability of streamflow response to climate change scenarios in a mesoscale basin, *J. Hydrol.*, 293, 255–269.

Francois, C., A. Quesney, and C. Ottle (2003), Sequential assimlation of ERS-1 SAR data into a coupled land surface-hydrological model using an extended Kalman filter, *Hydrometeorology*, *4*, 473–487.

Fusco, L., V. Guidetti, and J. van Bemmelen (2005), e-Collaboration and Grid-on-Demand computing for Earth Science at ESA, *ERCIM News*, *61*, 12–13.

Gupta, H. V., T. Wagener, and Y. Liu (2008), Reconciling theory with observations: Elements of a diagnostic approach to model evaluation, *Hydrol. Processes*, *22*, 3802–3813, doi:10.1002/hyp.6989.

Gupta, R. P., and S. Banerji (1985), Monitoring of reservoir volume using LANDSAT data, *J. Hydrol.*, *77*, 159–170.

Hagen, A. (2003), Fuzzy set approach to assessing similarity of categorical maps, *Int. J. Geogr. Inf. Sci.*, *17*, 235–249.

Henry, J. B., P. Chastanet, K. Fellah, and Y. L. Desnos (2006), ENVISAT multi-polarised ASAR data for flood mapping, *Int. J. Remote Sens.*, *27*(10), 1921–1929.

Hess, L. L., J. M. Melack, and D. S. Simonett (1990), Radar detection of flooding beneath the forest canopy: A review, *Int. J. Remote Sens.*, *11*, 1313–1325.

Hess, L. L., J. M. Melack, S. Filoso, and Y. Wang (1995), Delineation of inundated area and vegetation along the Amazon floodplain with the SIR-C synthetic aperture radar, *IEEE Trans. Geosci. Remote Sens.*, *33*(4), 896–904.

Hess, L. L., J. M. Melack, E. M. L. M. Novo, C. C. F. Barbosa, and M. Gastil (2003), Dual-season mapping of wetland inundation and vegetation for the central Amazon basin, *Remote Sens. Environ.*, *87*, 404–428.

Horritt, M. S. (1999), A statistical active contour model for SAR image segmentation, *Image Vision Comput.*, *17*(3), 213–224.

Horritt, M. S. (2006), A methodology for the validation of uncertain flood inundation models, *J. Hydrol.*, *326*, 153–165.

Horritt, M. S., and P. D. Bates (2002), Evaluation of 1D and 2D numerical models for predicting river flood inundation, *J. Hydrol.*, *268*, 87–99.

Horritt, M. S., D. C. Mason, and A. J. Luckman (2001), Flood boundary delineation from synthetic aperture radar imagery using a statistical active contour model, *Int. J. Remote Sens.*, *22*(13), 2489–2507.

Horritt, M. S., D. C. Mason, D. M. Cobby, I. J. Davenport, and P. D. Bates (2003), Waterline mapping in flooded vegetation from airborne SAR imagery, *Remote Sens. Environ.*, *85*(3), 271–281.

Horritt, M. S., G. Di Baldassarre, P. D. Bates, and A. Brath (2007), Comparing the performance of a 2D finite element and a 2D finite volume model of floodplain inundation using airborne SAR imagery, *Hydrol. Processes*, *21*, 2745–2759.

Hostache, R., C. Puech, and D. Raclot (2005), Caractérisation spatiale d'aléa inondation à partir d'images satellites radar: Cartographie et estimation de niveaux d'eau par fusion des données images avec des données topographiques, paper presented at International Conference on Spatial Analysis and Geomatics, UMR ESPACE, Avignon, France.

Hostache, R., P. Matgen, G. Schumann, C. Puech, L. Hoffmann, and L. Pfister (2009), Water level estimation and reduction of hydraulic model calibration uncertainties using satellite SAR images of floods, *IEEE Trans. Geosci. Remote Sens.*, *47*, 431–441.

Hunter, N. M. (2005), Development and assessment of dynamic storage cell codes for flood inundation modelling, Ph.D. thesis, Univ. of Bristol, Bristol, U. K.

Hunter, N. M., P. D. Bates, M. S. Horritt, P. J. De Roo, and M. Werner (2005), Utility of different data types for flood inundation models within a GLUE framework, *Hydrol. Earth Syst. Sci.*, *9*, 412–430.

Imhoff, M. L., C. H. Vermillion, M. Story, and F. Polcyn (1986), Space-borne radar for monsoon and storm induced flood control planning in Bangladesh: A result of the Shuttle Imaging Radar-B program, *Sci. Total Environ.*, *56*, 277–286.

Jin, Y.-Q. (1999), A flooding index and its regional threshold value for monitoring floods in China from SSM/I data, *Int. J. Remote Sens.*, *20*(5), 1025–1030.

Kiel, B., D. Alsdorf, and G. LeFavour (2006), Capability of SRTM C- and X-band DEM data to measure water elevations in Ohio and the Amazon, *Photogramm. Eng. Remote Sens.*, *72*, 313–320.

Kirchner, J. W. (2006), Getting the right answers for the right reasons: Linking measurements, analyses, and models to advance the science of hydrology, *Water Resour. Res.*, *42*, W03S04, doi:10.1029/2005WR004362.

Lane, S. N., and J. H. Chandler (2003), Editorial: The generation of high quality topographic data for hydrology and geomorphology: New data sources, new applications and new problems, *Earth Surf. Processes Landforms*, *28*, 229–230.

Lane, S. N., T. D. James, H. Pritchard, and M. Saunders (2003), Photogrammetric and laser altimetric reconstruction of water levels for extreme flood event analysis, *Photogramm. Record*, *18*(104), 293–307.

Laugier, O., K. Fellah, N. Tholey, C. Meyer, and P. De Fraipont (1997), High temporal detection and monitoring of flood zone dynamic using ERS data around catastrophic natural events: The 1993 and 1994 Camargue flood events, paper presented at 3rd ERS Symposium on Space at the Service of Our Environment, Eur. Space Agency, Florence, Italy.

LeFavour, G., and D. Alsdorf (2005), Water slope and discharge in the Amazon River estimated using the shuttle radar topography mission digital elevation model, *Geophys. Res. Lett.*, *32*, L17404, doi:10.1029/2005GL023836.

Leopold, L. B., and T. Maddock (1953), Hydraulic geometry of stream channels and some physiographic implications, *U.S. Geol. Surv. Prof. Pap.*, *252*.

Li, H., and J. Wu (2004), Use and misuse of landscape indices, *Landscape Ecol.*, *19*, 389–399.

Liu, Y., S. Nishiyama, and T. Yano (2004), Analysis of four change detection algorithms in bi-temporal space with a case study, *Int. J. Remote Sens.*, *25*(11), 2121–2139.

Lu, D., P. Mausel, E. Brondizio, and E. Moran (2004), Change detection techniques, *Int. J. Remote Sens.*, *25*(12), 2365–2407.

MacIntosh, H., and G. Profeti (1995), The use of ERS SAR data to manage flood emergencies at the smaller scale, paper presented at 2nd ERS Applications Workshop, Eur. Space Agency, London.

Madsen, H., and R. Canizares (1999), Comparison of extended and ensemble Kalman filter for data assimilation in coastal area modelling, *Int. J. Numer. Methods Fluids*, *31*, 961–981.

Madsen, H., and C. Skotner (2005), Adaptive state updating in real-time river flow forecasting—A combined filtering and error forecasting procedure, *J. Hydrol.*, *308*, 302–312.

Marcus, W. A., and M. A. Fonstad (2008), Optical remote mapping of rivers at sub-meter resolutions and watershed extents, *Earth Surf. Processes Landforms*, *33*, 4–24.

Marks, K., and P. Bates (2000), Integration of high-resolution topographic data with floodplain flow models, *Hydrol. Processes*, *14*, 2109–2122.

Mason, D. C., I. J. Davenport, R. A. Flather, and C. Gurney (1998), A digital elevation model of the inter-tidal areas of the Walsh, England, produced by the waterline method, *Int. J. Remote Sens.*, *19*(8), 1455–1460.

Mason, D. C., D. M. Cobby, M. S. Horritt, and P. D. Bates (2003), Floodplain friction parameterization in two-dimensional river flood models using vegetation heights derived from airborne scanning laser altimetry, *Hydrol. Processes*, *17*, 1711–1732.

Mason, D. C., M. S. Horritt, J. T. Dall'Amico, T. R. Scott, and P. D. Bates (2007), Improving river flood extent delineation from synthetic aperture radar using airborne laser altimetry, *IEEE Trans. Geosci. Remote Sens.*, *45*, 3932–3943.

Mason, D. C., P. D. Bates, and J. T. Dall'Amico (2009), Calibration of uncertain flood inundation models using remotely sensed water levels, *J. Hydrol.*, *368*, 224–236.

Matgen, P., J. B. Henry, F. Pappenberger, P. De Fraipont, L. Hoffmann, and L. Pfister (2004), Uncertainty in calibrating flood propagation models with flood boundaries observed from synthetic aperture radar imagery, paper presented at 20th ISPRS Congress, Int. Soc. for Photogramm. and Remote Sens., Istanbul.

Matgen, P., A. El Idrissi, J.-B. Henry, N. Tholey, L. Hoffmann, P. De Fraipont, and L. Pfister (2006), Patterns of remotely sensed floodplain saturation and its use in runoff predictions, *Hydrol. Processes*, 20(8), 1805–1825.

Matgen, P., G. Schumann, J. Henry, L. Hoffmann, and L. Pfister (2007a), Integration of SAR-derived inundation areas, high precision topographic data and a river flow model toward real-time flood management, *Int. J. Appl. Earth Obs. Geoinf.*, 9(3), 247–263.

Matgen, P., G. Schumann, F. Pappenberger, and L. Pfister (2007b), Sequential assimilation of remotely sensed water stages in flood inundation models, in *Symposium HS3007 at IUGG2007: Remote Sensing for Environmental Monitoring and Change Detection*, IAHS Publ., 316, 78–88.

McGinnis, D. F., and A. Rango (1975), Earth resources satellite systems for flood monitoring, *Geophys. Res. Lett.*, 2, 132–135.

Melack, J. M., L. L. Hess, M. Gastil, B. R. Forsberg, S. K. Hamilton, I. B. T. Lima, and E. M. L. M. Novo (2004), Regionalization of methane emissions in the Amazon basin with microwave remote sensing, *Global Change Biol.*, 10, 530–544.

Neal, J. C., P. M. Atkinson, and C. W. Hutton (2007), Flood inundation model updating using an ensemble Kalman filter and spatially distributed measurements, *J. Hydrol.*, 336, 401–415.

Neal, J., G. Schumann, P. D. Bates, W. Buytaert, P. Matgen, and F. Pappenberger (2009), An assimilation approach to discharge estimation from space, *Hydrol. Processes*, in press.

Oberstadler, R., H. Hönsch, and D. Huth (1997), Assessment of the mapping capabilities of ERS-1 SAR data for flood mapping: A case study in Germany, *Hydrol. Processes*, 10, 1415–1425.

Ottle, C., and D. Vidal-Madjar (1994), Assimilation of soil moisture inferred from infrared remote sensing in a hydrological model over the HAPEX-MOBILHY region, *J. Hydrol.*, 158, 241–264.

Papa, F., C. Prigent, W. B. Rossow, B. Legresy, and F. Remy (2006), Inundated wetland dynamics over boreal regions from remote sensing: The use of TOPEX-Poseidon dual-frequency radar altimeter observations, *Int. J. Remote Sens.*, 27(21), 4847–4866.

Pappenberger, F., and K. J. Beven (2006), Ignorance is bliss: Or seven reasons not to use uncertainty analysis, *Water Resour. Res.*, 42, W05302, doi:10.1029/2005WR004820.

Pappenberger, F., P. Matgen, K. Beven, J. B. Henry, L. Pfister, and P. De Fraipont (2006), Influence of uncertain boundary conditions and model structure on flood inundation predictions, *Adv. Water Resour.*, 29, 1430–1449.

Pappenberger, F., K. Frodsham, K. Beven, R. Romanowicz, and P. Matgen (2007), Fuzzy set approach to calibrating distributed flood inundation models using remote sensing observations, *Hydrol. Earth Syst. Sci.*, 11, 739–752.

Pauwels, V. R. N., R. Hoeben, N. E. C. Verhoest, and F. P. De Troch (2001), The importance of the spatial patterns of remotely sensed soil moisture in the improvement of discharge predictions for small-scale basins through data assimilation, *J. Hydrol.*, 251, 88–102.

Profeti, G., and H. Macintosh (1997), Flood management through LANDSAT TM and ERS SAR data: A case study, *Hydrol. Processes*, 11, 1397–1408.

Puech, C., and D. Raclot (2002), Using geographical information systems and aerial photographs to determine water levels during floods, *Hydrol. Processes*, 16, 1593–1602.

Raclot, D. (2006), Remote sensing of water levels on floodplains: A spatial approach guided by hydraulic functioning, *Int. J. Remote Sens.*, 27(12), 2553–2574.

Raclot, D., and C. Puech (2003), What does AI contribute to hydrology? Aerial photos and flood levels, *Appl. Artif. Intel.*, 17, 71–86.

Rees, W. G. (2001), *Physical Principles of Remote Sensing*, Cambridge Univ. Press, Cambridge, U. K.

Reichle, R. H., D. B. Mclaughlin, and D. Entekhabi (2002), Hydrologic data assimilation with the ensemble Kalman filter, *Mon. Weather Rev.*, 130, 103–114.

Romanowicz, R., K. J. Beven, and J. Tawn (1996), Bayesian calibration of flood inundation models, in *Floodplain Processes*, edited by M. G. Anderson, D. E. Walling, and P. D. Bates, pp. 333–360, John Wiley, New York.

Sanders, B. F. (2007), Evaluation of on-line DEMs for flood inundation modeling, *Adv. Water Resour.*, 30, 1831–1843.

Sanyal, J., and X. X. Lu (2004), Application of remote sensing in flood management with special reference to monsoon Asia: A review, *Nat. Hazards*, 33, 283–301.

Schumann, G., J. B. Henry, L. Hoffmann, L. Pfister, F. Pappenberger, and P. Matgen (2005), Demonstrating the high potential of remote sensing in hydraulic modelling and flood risk management, paper presented at Annual Conference of the Remote Sensing and Photogrammetry Society With the NERC Earth Observation Conference, Remote Sens. and Photogramm. Soc., Portsmouth, U. K.

Schumann, G., P. Matgen, F. Pappenberger, R. Hostache, and L. Pfister (2007a), Deriving distributed roughness values from satellite radar data for flood inundation modelling, *J. Hydrol.*, 344, 96–111.

Schumann, G., P. Matgen, F. Pappenberger, R. Hostache, C. Puech, L. Hoffmann, and L. Pfister (2007b), High-resolution 3D flood information from radar for effective flood hazard management, *IEEE Trans. Geosci. Remote Sens.*, 45, 1715–1725.

Schumann, G., P. Matgen, M. E. J. Cutler, A. Black, L. Hoffmann, and L. Pfister (2008a), Comparison of remotely sensed water stages from lidar, topographic contours and SRTM, *ISPRS J. Photogramm. Remote Sens.*, 63, 283–296.

Schumann, G., P. Matgen, and F. Pappenberger (2008b), Conditioning water stages from satellite imagery on uncertain data points, *IEEE Geosci. Remote Sens. Lett.*, 5, 810–813.

Schumann, G., P. Matgen, F. Pappenberger, A. Black, M. Cutler, L. Hoffmann, and L. Pfister (2008c), Evaluating uncertain flood inundation predictions with uncertain remotely sensed water stages, *Int. J. River Basin Manage.*, 6, 187–199.

Sippel, S. J., S. K. Hamilton, J. M. Melack, and E. M. M. Novo (1998), Passive microwave observations of inundation area and the area/stage relation in the Amazon River floodplain, *Int. J. Remote Sens.*, 19(16), 3055–3074.

Smith, L. C. (1997), Satellite remote sensing of river inundation area, stage, and discharge: A review, *Hydrol. Processes*, 11, 1427–1439.

Smith, L. C., and T. M. Pavelsky (2008), Estimation of river discharge, propagation speed, and hydraulic geometry from space: Lena River, Siberia, *Water Resour. Res.*, 44, W03427, doi:10.1029/2007WR006133.

Stanski, H. R., L. J. Wilson, and W. R. Burrows (1989), Survey of common verification methods in meteorology, *World Weather Watch Tech. Rep. 8*, World Meteorol. Organ., Geneva, Switzerland.

Straatsma, M. W., and H. Middelkoop (2006), Airborne laser scanning as a tool for lowland floodplain vegetation monitoring, *Hydrobiologia*, 565, 87–103.

Walker, J. P. (1999), Estimating soil moisture profile dynamics from near-surface soil moisture measurements and standard meteorological data, Ph.D. thesis, Dep. of Civ., Surv. and Environ. Eng., Univ. of Newcastle, Newcastle, N. S. W., Australia.

Walker, J. P., P. R. Houser, and R. H. Reichle (2003), New technologies require advances in hydrologic data assimilation, *Eos Trans. AGU*, 84, 545.

Werner, M., S. Blazkova, and J. Petr (2005a), Spatially distributed observations in constraining inundation modelling uncertainties, *Hydrol. Processes*, 19(16), 3081–3096.

Werner, M. G. F., N. M. Hunter, and P. D. Bates (2005b), Identifia-bility of distributed floodplain roughness values in flood extent estimation, *J. Hydrol.*, *314*, 139–157.

Wilson, M., P. Bates, D. Alsdorf, B. Forsberg, M. Horritt, J. Melack, F. Frappart, and J. Famiglietti (2007), Modeling large-scale inundation of Amazonian seasonally flooded wetlands, *Geophys. Res. Lett.*, *34*, L15404, doi:10.1029/2007GL030156.

Yu, D., and S. N. Lane (2006), Urban fluvial flood modelling using a two-dimensional diffusion-wave treatment, part I: Mesh resolu-tion effects, *Hydrol. Processes*, *20*, 1541–1565.

Zhou, C., J. Luo, C. Yang, B. Li, and S. Wang (2000), Flood monitoring using multi-temporal AVHRR and RADARSAT ima-gery, *Photogramm. Eng. Remote Sens.*, *66*, 633–638.

—————————

P. D. Bates and G. Schumann, School of Geographical Sciences, University of Bristol, University Road, Bristol BS8 1SS, UK. (guy.schumann@bristol.ac.uk)

M. S. Horritt, Halcrow Group Ltd., Swindon SN4 0QD, UK.

P. Matgen, Department of Environment and Agro-Biotechnologies, CRP–Gabriel Lippmann, L-4422 Belvaux, Luxembourg.

F. Pappenberger, European Centre for Medium-Range Weather Forecasts, Reading RG2 9AX, UK.